의학박사 학위논문

Exploring the mechanism of the hypoglycemic effect of metformin mediated by the gut microbiota and endogenous metabolites

장내 미생물 및 내인성 대사체 분석을 통한 메트포르민의 혈당 강하 기전 탐색

2022 년 2 월

서울대학교 대학원
협동과정 임상약리학전공
이 유 진

Ph.D. Dissertation of Medical Science

장내 미생물 및 내인성 대사체 분석을 통한 메트포르민의 혈당 강하 기전 탐색

Exploring the mechanism of the hypoglycemic effect of metformin mediated by the gut microbiota and endogenous metabolites

February 2021

Graduate School of Department of Medicine
Seoul National University
The Interdisciplinary Program of
Clinical Pharmacology Major
Yujin Lee

장내 미생물 및 내인성 대사체 분석을 통한 메트포르민의 혈당 강하 기전 탐색

지도 교수 조 주 연

이 논문을 의학박사 학위논문으로 제출함

2021 년 10 월

서울대학교 대학원
협동과정 임상약리학전공
이 유 진

이유진의 의학박사 학위논문을 인준함
2022 년 1 월

위 원 장 _____ (인)

부위원장 _____ (인)

위 원 _____ (인)

위 원 _____ (인)

위 원 _____ (인)

Exploring the mechanism of the hypoglycemic effect of metformin mediated by the gut microbiota and endogenous metabolites

Joo-Youn Cho

Submitting a Ph.D. Dissertation of
Medical Science

October 2021

Graduate School of Department of Medicine
Seoul National University
The Interdisciplinary Program of
Clinical Pharmacology Major

Yujin Lee

Confirming the Ph.D. Dissertation written by
Yujin Lee
January 2022

Chair _____ (Seal)

Vice Chair _____ (Seal)

Examiner _____ (Seal)

Examiner _____ (Seal)

Examiner _____ (Seal)

Abstract

Exploring the mechanism of the hypoglycemic effect of metformin mediated by the gut microbiota and endogenous metabolites

Yujin Lee

The Interdisciplinary Program of
Clinical Pharmacology Major
Graduate School of Department of Medicine
Seoul National University

Introduction: Metformin, the most widely used antidiabetic drug, is known to activate AMP-mediated protein kinase (AMPK) in the liver, thereby inhibiting the biosynthesis of fatty acids and production of glucose. Recently, as the mechanism of metformin through the gastrointestinal tract has emerged, interest in effects of gut microbiome on hypoglycemia is increasing. Several previous studies have shown that metformin alters the microbial composition in both animal and human, and suggested that the microbiota contributes to the hypoglycemic effect of metformin via modulation of microbial metabolites. However, the microbial functions on hypoglycemic effect

of metformin have not been elucidated. Therefore, in this study, two clinical trials were performed to explore various interactions between gut and the hypoglycemic effect of metformin. Finally, potential pathways that correlated with the hypoglycemic effects of metformin were suggested through metagenomics- and metabolomics approaches.

Methods: To evaluate effects of metformin on microbiome and metabolites, an open-label and single-arm clinical trial was performed in 20 healthy Korean male adults. The subjects received 1000 mg of oral metformin twice daily for 4 days. In addition, to assess impacts of gut environmental changes on the hypoglycemic effect of metformin, 14 healthy Korean males were involved in this four-period clinical study: baseline; metformin (i.e., multiple oral doses of 1000 mg metformin on day 1-2); cholestyramine (i.e., multiple oral doses of 4g cholestyramine on day 3-9); cholestyramine+metformin (i.e., multiple oral doses of 1000 mg metformin on days 8-9). In each period of two clinical trials, serum glucose and insulin concentrations, stool samples for gut microbial analysis, and plasma, urine, and stool samples for metabolomic analysis were obtained. Global metabolomics was performed using GC-TOFMS and network analysis was applied to explore potential pathway of the hypoglycemic effect.

Results: After metformin administration, the relative abundances of *Escherichia*, *Romboutsia*, *Intestinibacter*, and *Clostridium* were changed.

In addition, carbohydrates, amino acids, and fatty acids were altered. These alterations in microbiome and metabolites were correlated with the hypoglycemic effect of metformin. After cholestyramine administration, the relative abundances of *Rothia* and *Veillonella* were increased. Additionally, microbial metabolites such as bile acids and short-chain fatty acids were altered. The alterations in microbiome and microbial metabolites reduced to the pharmacodynamics of metformin and affected to profiles of endogenous metabolites changed by metformin administration. Furthermore, energy metabolism, branched-chain amino acid metabolism, and purine metabolism were suggested as major metabolic pathways related to the hypoglycemic effect of metformin.

Conclusions: These studies indicated that specific alterations in both microbiome and metabolites affected to the hypoglycemic effect of metformin. The alterations impacted host metabolism, which is correlated with hypoglycemia. In particular, energy metabolism, branched-chain amino acids metabolism, and purine metabolism were related to the hypoglycemic effect of metformin. The results will help uncover the potential underlying mechanisms of metformin within the gastrointestinal tract.

* Part of this work has been published in Diabetes Research and Clinical Practice (Yujin Lee et al. *Diabetes Research and Clinical Practice* 178 (2021): 108985).

Keyword: Metformin, Type 2 diabetes, Microbiome, Metabolomics, Pharmacodynamics

Student Number: 2017-20297

Table of contents

List of figures

List of tables

Introduction

Metformin is the most widely used antidiabetic drug for treating patients with type 2 diabetes (T2D) and is recommended as a first-line therapy due to its specific hypoglycemic effect, relative safety, and low cost [1, 2].

Metformin is known to induce glucose utilization and reduce gluconeogenesis through the activation of AMP-mediated protein kinase (AMPK) in the liver by entering hepatocytes through organic cation transporter 1 (OCT1) [3, 4]. By activating AMPK, the activity of enzymes involved in the biosynthesis of fatty acids is reduced, and glucose production is inhibited [4].

Metformin is an orally administered drug that is absorbed in the small intestine. The absolute oral bioavailability of metformin is approximately 40 to 60% [5]. In addition, the concentration of metformin in the human intestine is typically 30-300 times higher than that of plasma [6], and a study using [^{11}C]metformin positron emission tomography (PET) showed that the concentration of orally administered metformin was high in the intestines [3]. A previous study showed that metformin administered intravenously to rats and humans had fewer hypoglycemic effects than oral dosing [7, 8]. Thus, the

possibility cannot be excluded that the intestine is an essential organ involved in the effect of metformin to improve hyperglycemia.

The intestines play a number of roles in regulating blood glucose levels, such as secreting glucagon-like peptide 1 (GLP1) and peptide YY, regulating bile acid metabolism, and affecting the growth and composition of the gut microbiome [9, 10]. Some studies have shown that metformin can change the microbial composition [1, 2, 11] and have suggested that the microbiota contributes to the hypoglycemic effect of metformin via the modulation of microbial metabolites, including bile acids and short chain fatty acids (SCFA) [12]. The primary bile acids, which are cholesterol-derived metabolites, are transformed into secondary bile acids by enteric anaerobic bacteria. The bile acids are involved in the regulation of glucose metabolism in the liver and small intestine by binding to nuclear receptors, including farnesoid X receptor (FXR) and Takeda G protein-coupled receptor 5 (TGR5) [13]. Some previous studies showed that cholic acid decreased the expression of the gluconeogenic genes, including phosphoenolpyruvate kinase (PEPCK), glucose-6-phosphatase, and fructose-1,6-bisphosphatase, through FXR activation [14, 15]. In line with this finding, obeticholic acid decrease insulin resistance through activation of FXR signaling [16]. Therefore, the bile acids certainly impact regulation of glucose homeostasis.

Short chain fatty acids (SCFA), one of the other microbial metabolites, are fermentation products of diets that are undigested in the gut and are produced by SCFA-producing microbiota such as *Shewanella* (*Proteobacteria*) and *Blautia* (*Firmicutes*) [1, 17]. Previous works demonstrated that the increase in production of the SCFA triggers intestinal gluconeogenesis in mice [11] and abnormalities in the production or absorption of SCFA were correlated with an increased risk of T2D [18].

Some previous studies showed that changes in microbiome and their metabolites were correlated with the hypoglycemic effect of metformin. However, the exact microbial genus and microbial metabolites that are related to the hypoglycemic effect and how these are responsible for the hypoglycemic effect of metformin remain undefined.

Therefore, two clinical studies were performed to explore various interactions between the gut and the hypoglycemic effect of metformin. The first study was conducted to identify changes in microbiome and metabolites after metformin administration. The second study was conducted to explore the effects of gut environmental changes on the hypoglycemic effect. These studies indicated that metformin altered specific microbiota and metabolites and that the hypoglycemic effect was affected by changes in the intestinal environment. Finally, to explain the mechanism of metformin in the intestine, potential pathways

that correlated with the hypoglycemic effect of metformin were suggested through metagenomics and metabolomics approaches.

Methods

Subjects

STUDY Ⅰ

This study aimed to recruit 20 healthy adult male subjects who were 19–45 years old and had a body mass index (BMI) of 18.0–28.0 kg/m^2 during the screening visit. Subjects with active or a history of clinically significant diseases of the kidney or the digestive, nervous, endocrine, or immune systems were excluded from the study. In addition, subjects with a history of gastrointestinal disorders or surgery that could affect the absorption of metformin were also excluded. Subjects with defecation less than five times a week or more than three times a day or who had excessively hard or soft stools were excluded from the study. Subjects whose blood aspartate aminotransferase (AST) and alanine aminotransferase (ALT) values exceeded 1.5 times the upper limit of the normal range during the screening visit or whose estimated glomerular filtration rate (eGFR) calculated by the Modification of Diet in Renal Disease (MDRD) was less than 80 mL/min/1.73 m2 were also excluded.

STUDY Ⅱ

This study aimed to include 15 healthy adult male subjects who were 19–50 years old and had a BMI of 18.0–28.0 kg/m^2 during the screening visit, and 14 subjects completed the entire study. Subjects with active or a history of clinically significant diseases of the liver or the kidney, digestive, nervous, endocrine, or immune systems were excluded from the study. In addition, subjects with a history of gastrointestinal disorders or surgery that could affect the absorption of drugs were also excluded. Subjects with defecation less than five times a week or more than three times a day or who had excessively hard or soft stools were excluded from the study. Subjects with genetic problems such as galactose intolerance, lactase deficiency or glucose–galactose malabsorption were excluded. Also, subjects whose blood AST and ALT values exceeded 2 times the upper limit of the normal range during the screening visit or whose eGFR calculated by the MDRD was less than 80 mL/min/1.73 m^2 were excluded.

Study design

STUDY Ⅰ①

① Clinical trial (study Ⅰ) was performed by Eunwoo Kim and Prof. Jae–Yong Chung

This was an open-label, single-arm study (Figure 1). The subjects received the first dose of 500 mg of oral metformin on day 1 at 9 a.m. for the safety of the subjects, and then they received 1000 mg twice daily from day 1 (1 d, 1:30 p.m.) to day 4 (4 d) in the morning. Plasma samples for the pharmacodynamics (PD) evaluation of metformin were collected before the first metformin dose (baseline) and on day 4 after the last metformin dose (metformin period). Stool samples for metagenomics were collected on the morning of day 1 before the first metformin dose and on day 4 after the last metformin dose. The sample used for analysis was from the first stool in the morning. Urine samples were collected on day −1 and day 4. Additionally, plasma, stool, and urine samples were used for untargeted metabolomic analysis.

The subjects were provided with a normal diet, not a high-fat, high-fiber diet, that met the recommended daily caloric intake of approximately 2700 kcal for adult men, and they were limited the intake of foods containing lactic acid bacteria, grapefruit, and caffeine. In addition, they were asked to eat the full amount of the meal during hospitalization, and any meals other than the provided meals were prohibited.

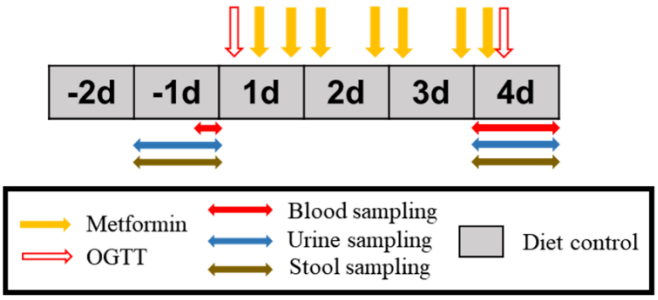

Figure 1. Study design of part 1 study.

STUDY Ⅱ[②]

This was an open-label, single center study. The study consisted of four periods, which were baseline (-1d or 1d, baseline of metformin period), metformin (2d), cholestyramine (8d, baseline of cholestyramine+metformin period), and cholestyramine+metformin (9d), according to the treatment given in each period (Figure 2). The subjects were admitted to the clinical trial center at Seoul National University Bundang Hospital one day before administration of the clinical trial drugs (day -1). Then, the subjects received the first dose of 500 mg of oral metformin on day 1 at 1:30 p.m. for the safety of the subjects, and then they received 1000 mg once daily from day 1 (1 d, 9 p.m.) to day 2 (2 d) in the morning. After the washout period, the

② Clinical trial (study Ⅱ) was performed by Deok Yong Yoon and Prof. Jae-Yong Chung

subjects administered 4g of cholestyramine 3 times a day with meals from day 3 to day 9 in the morning. Metformin was administered again from day 8 to day 9 in the same manner as on day 1 to day 2.

Plasma samples for the PD evaluation of metformin were collected before the first metformin dose (baseline, 1d), on day 2 after the last metformin dose (metformin period, 2d), on day 8 after administration of cholestyramine alone (cholestyramine period, 8d), and on day 9 after the last metformin dose (cholestyramine+metformin period, 9d). Stool samples for metagenomics were collected on the morning of day 1 and on day 8. The sample used for analysis was from the first stool in the morning. 12h-interval urine samples were collected on day -1, 1, 7, and 8. Additionally, plasma, stool, and urine samples were used for global metabolomics.

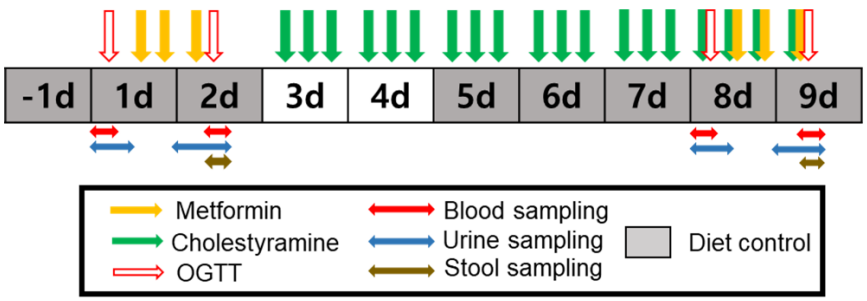

Figure 2. Study design of part 2 study.

Pharmacodynamic (PD) assessments of metformin

STUDY I

For PD evaluation of metformin, an oral glucose tolerance test (OGTT) was performed, and the serum insulin concentration was measured at baseline (before the first dose of metformin) and metformin period (2 hours after the last dose of metformin) (Supplementary Figure 1). In brief, a solution containing 75 g glucose was administered to the subjects on an empty stomach, and samples for determining the serum glucose concentration were collected at 0 (before administration of the solution containing 75 g glucose), 0.25, 0.5, 0.75, 1, 1.5, and 2 h. The serum insulin concentration was measured only at 0 h (before administration of the solution containing 75 g glucose).

To evaluate glucose parameters, the maximum serum glucose concentration (G_{max}) was presented as the actual observed value, and the area under the glucose curve (AUGC) was calculated by the linear-linear trapezoidal method. Homeostatic model assessment of insulin resistance (HOMA-IR) was calculated as (glucose · insulin)/405.

The baseline corrected PD parameters, including ΔG_{max}, ΔAUGC, and ΔHOMA-IR, after the last metformin administration were defined by subtracting the baseline values from the metformin values (i.e., G_{max} at metformin period - G_{max} at baseline). Smaller ΔAUGC, ΔG_{max}, and

ΔHOMA−IR values, i.e., larger absolute values of the parameters, were interpreted as stronger effects of metformin treatment. The PD parameters were confirmed whether the data had a normal distribution through a normality test. Then, the paired t test was used for G_{max} and AUGC, and the Wilcoxon signed rank test was used for HOMA−IR, with significance determined at the level of 0.05. Statistical analysis was performed using GraphPad Prism 7 (GraphPad Software, Inc., San Diego, CA, USA).

STUDY Ⅱ

An OGTT was performed for PD evaluation, and the serum insulin concentration was measured at each of the four periods. A solution containing 75 g glucose was administered to the subjects on an empty stomach, and samples for determining the serum glucose concentration were collected at 0 (before administration of the solution containing 75 g glucose), 0.25, 0.5, 0.75, 1, 1.5, and 2 h. The serum insulin concentration was measured only at 0 h.

To evaluate glucose parameters, the maximum serum glucose concentration (G_{max}) was presented as the actual observed value, and the area under the glucose curve (AUGC) was calculated by the linear−linear trapezoidal method. Homeostatic model assessment of insulin resistance (HOMA−IR) was calculated as (glucose · insulin)/405.

The baseline corrected PD parameters, including ΔG_{max} and ΔAUGC, after metformin administration were defined by subtracting the baseline values from that of the metformin period (i.e., G_{max} at metformin period – G_{max} at baseline), and subtracting the values of cholestyramine period from that of the cholestyramine+metformin period. Smaller ΔAUGC and ΔG_{max} values, i.e., larger absolute values of the parameters, were interpreted as stronger hypoglycemic effects of metformin treatment. The PD parameters were confirmed whether the data had a normal distribution through a normality test. Then, the Wilcoxon test was used for HOMA-IR and the paired t test was used for G_{max}, AUGC, ΔG_{max}, and ΔAUGC with significance determined at the level of 0.05.

The pharmacodynamics parameters were obtained by non-compartmental methods with Phoenix® WinNonlin® software version 8.0 (Certara USA Inc., Princeton, NJ, USA). In addition, statistical analysis was performed using GraphPad Prism 7 (GraphPad Software, Inc., San Diego, CA, USA).

Analysis of the gut microbiome

STUDY Ⅰ③

③ 16S rRNA sequencing (study Ⅰ) was performed by DNA Link, Inc

Stool samples were collected from all the recruited subjects for 16S rRNA sequencing. The samples were mixed using a 3M sample mixer, dispensed into Eppendorf tubes and frozen at −70° C until analysis.

DNA was extracted from the stool samples using the PowerSoil® DNA Isolation Kit, and amplification of the 16S rRNA gene was conducted using the 16S V3−V4 primers. Normalization and pooling of the final product were performed using PicoGreen. The size of the libraries was verified using TapeStation DNA ScreenTape D1000 (Agilent), and sequencing was performed using the MiSeq™ platform (Illumina, San Diego, USA). Taxonomic profiling was performed using a module of MicrobiomeAnalyst for marker data profiling.

The alpha diversity (within−sample diversity, species eveness) is presented as the Shannon index, and the Kruskal−Wallis test was performed for comparisons between periods. The beta diversity (between−sample diversity, community dissimilarity) is presented on a principal coordinate analysis (PCoA) plot, and Bray−Curtis dissimilarity was evaluated by permutational multivariate analysis of variance (PERMANOVA). Significantly different genera between periods were identified by linear discriminant analysis (LDA) effect size (LEfSe) analysis, and the data were subjected to total sum normalization. This treatment yielded a relative proportional value for each feature by dividing each count of each feature by the size of the

total library, which eliminated bias related to different sequencing depths. The cutoffs for the false discovery rate (FDR)-adjusted p-value and LDA scores were 0.05 and 2.0, respectively. The change induced in the gut microbiome by metformin administration was identified through comparison between baseline and metformin periods.

STUDY Ⅱ④

The Illumina next generation sequencing (NGS) was performed in each stool samples. For library construction, DNA/RNA is extracted from samples and performing quality control (QC), qualified samples proceed to library construction. The sequencing library is prepared by random fragmentation of the DNA or cDNA sample, followed by 5' and 3' adapter ligation. Alternatively, "tagmentation" combines the fragmentation and ligation reactions into a single step that greatly increases the efficiency of the library preparation process. Adapter-ligated fragments are the PCR amplified and gel purified. For cluster generation, the library is loaded into a flow cell where fragments are captured on a lawn of surface-bound oligos complementary to the library adapters. Each fragment is then amplified into distinct, clonal

④ 16S rRNA sequencing (study Ⅱ) was performed by Macrogen, Inc

clusters through bridge amplification. When cluster generation is complete, the templates are ready for sequencing. Then, sequencing data is converted into raw data for the analysis. Also, Taxonomic profiling was performed using a module of MicrobiomeAnalyst for marker data profiling.

The alpha diversity is presented as the observed features and Shannon index. Also, the Mann-Whitney test was performed for comparisons between periods. The beta diversity is presented on a PCoA plot, and Bray-Curtis dissimilarity was evaluated by PERMANOVA. Significantly different genera between periods were identified by LEfSe analysis, and the data were subjected to total sum normalization. This treatment yielded a relative proportional value for each feature by dividing each count of each feature by the size of the total library, which eliminated bias related to different sequencing depths. The cutoffs for the FDR-adjusted p-value and LDA scores were 0.1 and 2.0, respectively. The change induced in the gut microbiome by cholestyramine administration was identified through comparison between metformin period and cholestyramine+metformin period.

Chemicals

The fatty acid methyl ester mixture (FAME) used for the relative retention time index and the authentic standards used for the identification of significant metabolic markers were purchased from Sigma-Aldrich (St. Louis, MO, USA). The extraction solvents used for sample preparation, such as isopropanol, acetonitrile, and water (HPLC grade), were obtained from J.T. Baker Chemical Co. (Phillipsburg, NJ, USA). Pyridine, methoxamine hydrochloride (MeOX), and N-methyl-N-(trimethylsilyl) trifluoroacetamide (MSTFA) were used for derivatization and purchased from Sigma-Aldrich. For quantification of plasma bile acids, Biocrates® Bile Acid Kit was purchased from Biocrates Life Science AG. For quantification of stool bile acids, deoxycholic acid (DCA), lithocholic acid (LCA), deoxycholic acid-d_4 (DCA-d_4), and lithocholic acid-d_4 (LCA-d_4) were purchased from Sigma-Aldrich. All the SCFAs including acetic acid, propionic acid, butyric acid, and valeric acid were purchased from Sigma-Aldrich. Acetic acid-d_4, hydrochloric acid (HCl, 37%), and *tert*-methyl butyl ether (MTBE) were also obtained from Sigma-Aldrich. Butyric acid-d_7 was obtained from Cayman Chemical (MI, USA).

Sample preparation for metabolomic analysis

For untargeted metabolomic analysis, all the samples were prepared using a protocol from a previous study with minor modifications. Frozen plasma, urine, and stool samples were thawed on ice, and quality control (QC) samples, made by pooling equal volumes (100 μL of the 1st extracted solution) of each sample, were used to validate the stability of the analytical performance and perform data filtering. For preparation of the plasma and urine samples, a 50 μL sample was extracted using 1 mL of N_2-degassed 1st extraction solution (3:3:2, acetonitrile:isopropanol:H_2O). For preparation of the stool sample, the 1st extraction solution was spiked into the stool sample at a sample mass to solution volume ratio of 50 mg of stool sample to 1 mL of the 1st extraction solution. Then, the samples were mixed for 15 min and centrifuged for 10 min at 18945 RCF and 4℃. Four hundred microliters of the supernatant was dried using a SpeedVac for 6 hours at 45℃ and 5.1 vacuum pressure. The dried samples were re-extracted with 400 μL of N_2-degassed 2nd extraction solution (1:1, acetonitrile: H_2O). Then, the extracted samples were redried using a SpeedVac for 8 hours under the same℃ onditions used in the first extraction step. The dried samples were derivatized with methoxyamine (20 mg/mL in pyridine) at 30℃ for 90 min and subsequently trimethylsilylated with a mixture

of fatty acid methyl ester (used for the retention time index) in N-methyl-N-(trimethylsilyl)-trifluoroacetamide at 70℃ for 45 min. Finally, 1 μL of the prepared samples was split-injected into an Agilent 7890 series gas chromatography system (Agilent, Santa Clara, CA) coupled to a time-of-flight mass spectrometer (LecoCorp., St. Joseph, MI, USA) (GC-TOFMS) for untargeted metabolomics analysis.

Plasma bile acid quantification was performed using the Biocrates® Bile Acid Kit (Biocrates Life Science AG, Innsbruck, Austria) with SCIEX liquid chromatography tandem mass spectrometry (AB Sciex API 4000™) according to the manufacturer's instruction.

For stool bile acid, 500mg of each wet stool samples were deproteinized with 450 μL ice-cold methanol. The samples were sonicated for 15 min and shaken for 20 min at room temperature. After shaking, the samples were centrifuged for 20 min at 18945 RCF and 4℃. The supernatants were diluted with methanol (1:200, v/v) and then they were diluted again with 30% methanol (1:1, v/v). Ten-microliter of internal standards were spiked into the diluted samples. The analysis of samples were performed using an Agilent 1260 Infinity II Prime (Agilent Technologies, California, USA) coupled to an Agilent 6460 Triple Quad Mass Spectrometer equipped with an ESI source. The ion detection was performed in negative mode and also the multiple reaction-monitoring mode (MRM) was used. The mobile phases

consisted of 5mM ammonium acetate (A) and methanol (B) at 40:60 (v/v). The composition of mobile phases was gradually changed; at the initial state of ammonium acetate–methanol (40:60, v/v) was held for 12 min, the gradient was changed to 30:70 (v/v) for 12.2–17min and it returned to its initial conditions 40:60 (v/v) for 17.2–20 min. The total run time was 20min and the flow rate was 0.3 mL/min with an injection volume of 5 μL.

For SCFAs quantification, stool was weighed 50 ± 20 mg and homogenized using water (1:10 ratio). Then, both ten-microliters of 1.0 M HCl and internal standard (IS) mixtures were spiked into 100 μL of plasma and homogenized stool samples. The samples were extracted by 200 μL of MTBE and the extracted samples were analyzed using 7000C mass spectrometer (Agilent, CA, USA) coupled with a 7890B gas chromatography (Agilent, CA, USA).

Untargeted metabolomic data analysis

For untargeted metabolomic data, Chroma TOF version 4.72 (LECO Corporation, MI, USA) was used for peak extraction, peak alignment, peak deconvolution, and peak identification. Data processing and multivariate analysis were performed using MetaboAnalyst 4.0. Detected metabolic features with greater than 50% missing values were

removed, and then, the metabolic features were filtered out according to a relative standard deviation of greater than 30% in the QC samples. The filtered metabolic features were normalized by sum, and Pareto scaling was applied for multivariate analysis.

Statistical analyses

The metabolic markers were selected using a paired t-test with a p-value and FDR adjusted p-value cutoff value of less than 0.05 in study 1 and study 2 studies, respectively. Pearson correlation and Spearman correlation analyses were performed after the normality test. Statistical analysis and correlation analysis were performed in GraphPad Prism 7 (GraphPad Software, Inc., San Diego, CA, USA) and R (v. 4.1.1).

Identification of metabolic markers

For metabolic marker identification, the online HMDB database (https://hmdb.ca/) and three commercially available libraries (NIST, LECO-Fiehn Rtx5, and Wiley 9) were used. After matching the mass fragments of the markers with the libraries, authentic standards were analyzed to compare the mass fragments. Then, the retention times of the markers and the standards were compared by calculating the

relative retention index. A network diagram was generated by using MetaMapp and Cytoscape (version 3.5).

Correlation analysis

STUDY Ⅰ

Pearson correlation and Spearman correlation analyses were performed after the normality test. Spearman correlation analysis was performed between the relative abundance of the microbiome and metabolic markers and between the abundance of the microbiome and PD parameters ($\triangle G_{max}$, $\triangle$AUGC, and $\triangle$HOMA-IR). Pearson correlation analysis was performed between the relative abundance of metabolic markers and PD parameters. Correlation analyses were performed using GraphPad Prism 7 (GraphPad Software, Inc., San Diego, CA, USA), and the p-value cutoff was 0.05.

STUDY Ⅱ

The correlation analyses were performed after the normality test. We applied Spearman correlation among the relative abundance of the microbiome, metabolic markers, and PD parameters. The correlation analyses were performed using Corrplot package in R (v. 4.1.1), and the p-value cutoff was 0.05.

Safety

All subjects were tested for vital signs, physical examinations, and clinical laboratory tests. All adverse events (AEs) were collected by the investigator and the subjects. Each AE was classified based on the first dose at each period. For example, AEs that occurred after the first administration of metformin and before the first administration of cholestyramine were classified as AEs of metformin period. All AEs were monitored and assessed by the investigators to determine their severity and relationship to the study drugs.

Results

STUDY Ⅰ. Microbial changes influence the hypoglycemic effect of metformin through the altered metabolic pathways.

Demographics

A total of 20 healthy adult male subjects were enrolled in this study, and all subjects completed the entire study. The mean ± standard deviation (SD) of the baseline demographic characteristics were followed: age, 24.85 ± 3.51 years; height, 176.0 ± 4.66 cm; weight, 73.43 ± 9.53 kg; BMI, 23.66 ± 2.72 kg/m^2.

Glucose parameters and PD parameters indicated the hypoglycemic effect of metformin

PD parameters of metformin according to glucose parameters, such as the values of G_{max}, AUGC, and HOMA-IR were evaluated. The serum glucose levels after the OGTT at baseline and metformin periods are presented in Figure 3. The G_{max} values of baseline and metformin periods were 169.1 ± 19.68 mg/dL and 138.1 ± 15.43 mg/dL,

respectively. The AUGC values of the baseline and metformin periods were 287.2 ± 36.29 h·mg/dL and 235.8 ± 26.17 h·mg/dL, respectively. The G_{max} and AUGC values were significantly decreased after metformin administration. However, the HOMA-IR value did not show a statistically significant change (p-value=2.71E-06 for G_{max}; 4.74E-06 for AUGC; 0.0539 for HOMA-IR) (Table 1). The values of the PD parameters, including $\triangle G_{max,}$ $\triangle$AUGC, and $\triangle$HOMA-IR, are listed in Table 1.

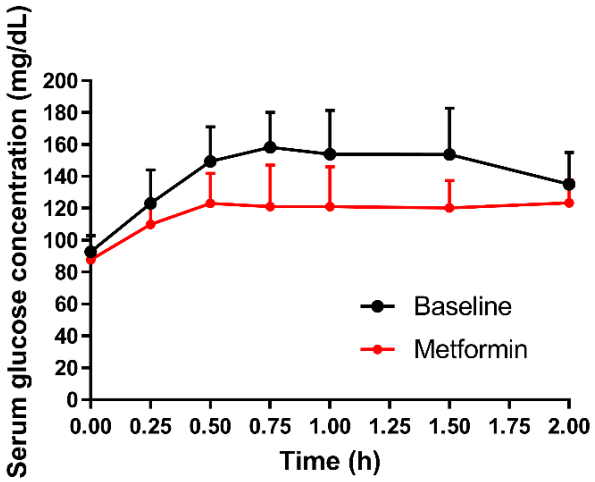

Figure 3. Mean serum glucose concentration-time profiles at baseline and metformin periods. Bars represent standard deviations. Meformin, after the last metformin dose.

Table 1. Glucose parameters and Pharmacodynamic parameters of metformin.

Parameter	Baseline	Metformin	p-value
G_{max} (mg/dL)	169.1 ± 19.68	138.1 ± 15.43	2.71E-06
AUGC (h·mg/dL)	287.2 ± 36.29	235.8 ± 26.17	4.74E-06
HOMA-IR	2.745 ± 3.944	1.529 ± 0.3737	0.0539
$\triangle G_{max}$ (mg/dL)	−31.05±19.69		-
△AUGC (h·mg/dL)	−51.41±34.11		-
△HOMA-IR	−1.22±3.840		-

Data are presented as the arithmetic mean ± standard deviation. G_{max}, maximum glucose concentration; AUGC, area under the glucose concentration curve from time 0 to the last measurable time point; HOMA-IR, homeostatic model assessment of insulin resistance.
The paired t test was used for G_{max} and AUGC. The Wilcoxon signed rank test was used for HOMA-IR.

Metformin affected to the gut microbial composition

Difference in relative abundance of gut microbiome at the genus level was observed between baseline and metformin periods. The relative abundances were changed after administration of metformin. The alpha diversity, which represented the species evenness in the samples, was significantly increased in the metformin period (Kruskal-Wallis test, p-value=0.043) (Figure 4a). A beta diversity showed significantly higher in the metformin period than at baseline (PERMANOVA, p-value < 0.004), indicating a more heterogeneous genus composition at the metformin period than at baseline (Figure 4b).

LEfSe analysis, for determining both statistical and biological relevance, was used for microbial biomarker discovery (FDR adjusted p−value < 0.05, linear discriminant analysis (LDA) score > 2.0). As a result, four microbiota were significantly changed after metformin administration. The relative abundances of *Intestinibacter*, *Clostridium*, and *Romboutsia* were decreased in the metformin period compared to those at baseline, whereas the abundance of *Escherichia* was increased in the metformin period (Figure 4c).

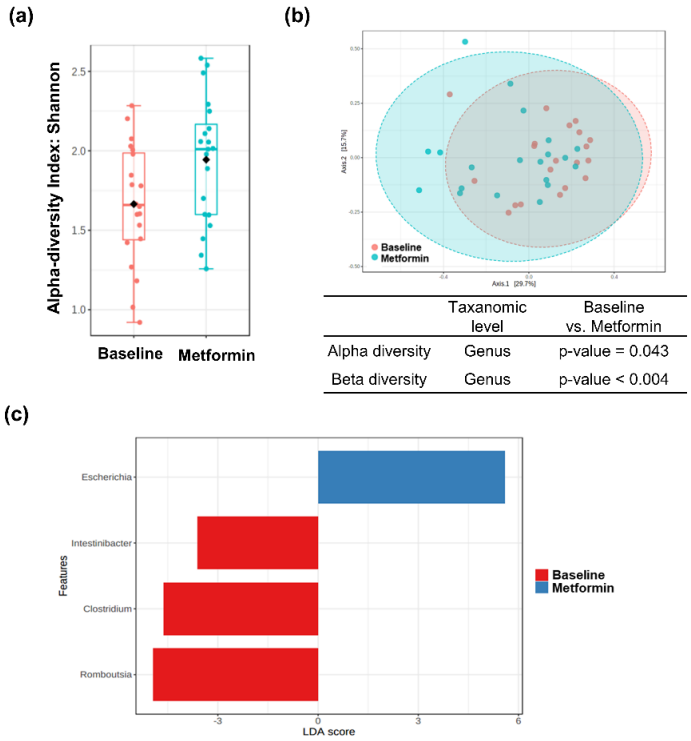

Figure 4. Metformin changed the composition of the gut microbiota. (a) Alpha diversity (Shannon index) and (b) PCoA plot were represented. (c) Microbiota that changed by metformin represented at the genus level (FDR adjusted p−value < 0.05, LDA score > 2.0). Histogram

showing the genera of bacteria that were more abundant at baseline (red color) or metformin period (blue color). Box plots showing medians as well as the lower and upper quartiles. Each dot represents an individual sample.

Hypoglycemic effect was related to gut microbial changes

To confirm whether the hypoglycemic effect of metformin was correlated with the microbial changes, correlation analysis was performed between the PD parameters and the relative abundance of altered microbiome at the phylum and genus levels (Figure 5). At the phylum level, *Firmicutes* was negatively correlated with the PD parameters. Conversely, *Proteobacteria* was positively correlated with the parameters (Figure 5a). Furthermore, at the genus level, the $\triangle G_{max}$ and △AUGC values were positively correlated with *Escherichia*. However, the PD parameters were negatively correlated with *Intestinibacter*, *Clostridium*, and *Romboutsia* (Figure 5b).

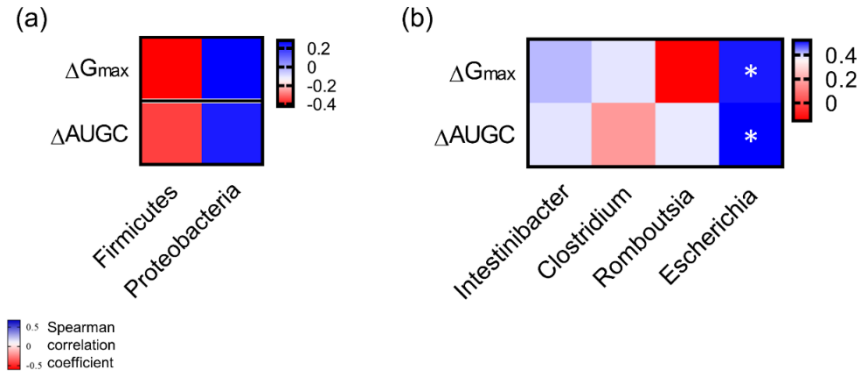

Figure 5. Spearman correlation analysis of the pharmacodynamic parameters (PDs) of metformin and the relative abundance of microbiome (a) at the phylum level and (b) at the genus level. The y-axis represents PDs, and the x-axis represents microbial taxa. Each square shows the correlation coefficient value. Blue color indicate a positive correlation, and red color indicate a negative correlation. *p-value < 0.05.

Metformin treatment altered metabolic profiling

Metabolites that altered after administration of metformin were analyzed as key drivers between the hypoglycemic effect and microbiome. Untargeted metabolomic analysis of urine, stool, and plasma samples was performed to identify changed metabolites between baseline and metformin periods. The reliability of the analytical performance and the quality of the data were validated by using QC samples that were tightly clustered in a plot of the principal component analysis (PCA) score derived from the urine, stool, and plasma metabolites (Figure 6). Twenty five urine, 10 stool, and 4

plasma metabolites were significantly changed after metformin administration (Table 2). All urinary amino acids were decreased at the metformin period. Also, most urinary carbohydrates and stool carbohydrates were decreased. Fatty acid such as palmitoleic acid were decreased in the metformin period. Furthermore, 13 urine, 4 stool, and 1 plasma metabolites were classified as microbial metabolite. Also, most microbial metabolites were decreased in the metformin period, as listed in Table 2.

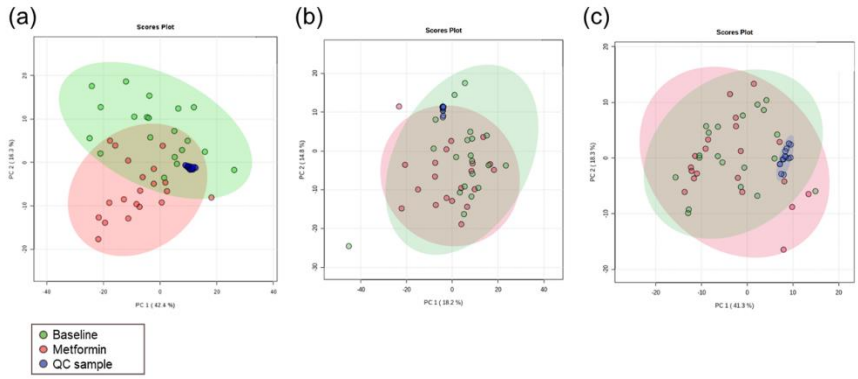

Figure 6. Principal component analysis (PCA) score plots of the baseline and metformin periods. PCA score plot of the (a) urinary metabolome, (b) stool metabolome, and (c) plasma metabolome. Green circles: baseline, red circles: metformin, and blue circles: quality control (QC) samples.

Table 2. List of changed metabolic markers from all samples between the baseline and metformin groups.

Name	p-value	FDR adjusted p-value	Fold change	Class
Urine				
†Scyllo-inositol	0.006	0.024	0.830	Alcohols
Serine	< 0.001	< 0.001	0.661	Amino acids
†Pyroglutamic acid	< 0.001	< 0.001	0.772	Amino acids
Threonine	< 0.001	< 0.001	0.520	Amino acids
Alanine	< 0.001	< 0.001	0.642	Amino acids
Glycine	< 0.001	0.001	0.668	Amino acids
† β-Alanine	< 0.001	0.002	0.781	Amino acids
†Valine	0.001	0.007	0.830	Amino acids
Lysine	0.018	0.055	0.558	Amino acids
Phenylalanine	0.019	0.057	0.861	Amino acids
†Hippuric Acid	< 0.001	< 0.001	5.692	Benzoic acids
Glyceric acid	< 0.001	< 0.001	0.639	Carbohydrates
D-Galactose	< 0.001	< 0.001	0.138	Carbohydrates
Ribonic acid	< 0.001	0.001	0.815	Carbohydrates
†D-Glucuronic acid	< 0.001	0.002	0.854	Carbohydrates
†Threonic acid	< 0.001	0.005	0.838	Carbohydrates
1,5-Anhydrosorbitol	< 0.001	0.005	1.213	Carbohydrates
Adonitol	0.006	0.025	0.839	Carbohydrates

2,3-Dihydroxybutanoic acid	0.014	0.045	1.383	Hydroxy acids
†2,4-Dihydroxybutyric acid	< 0.001	< 0.001	0.683	Hydroxy acids
†Glycolic acid	< 0.001	< 0.001	0.673	Hydroxy acids
†Lactic acid	< 0.001	0.003	0.570	Hydroxy acids
†3,4-Dihydroxybutyric acid	0.002	0.011	0.793	Hydroxy acids
†3-Hydroxyisobutyric acid	0.001	0.004	0.644	Hydroxy acids
†Hypoxanthine	< 0.001	< 0.001	2.197	Purines
Feces				
†Pipecolic acid	< 0.001	0.005	0.435	Amino acids
Phenylalanine	0.020	0.163	1.695	Amino acids
L-Serine	0.011	0.115	0.565	Amino acids
†L-Isoleucine	0.038	0.241	1.365	Amino acids
Glyceric acid	0.006	0.086	0.620	Carbohydrates
Glucose	0.002	0.051	0.609	Carbohydrates
D-Fructose	0.013	0.120	0.406	Carbohydrates
†Palmitoleic acid	0.026	0.207	0.595	Fatty acids
†Glycolic acid	0.004	0.071	0.630	Hydroxy acids
4-(Dimethylamino)butanoic acid	0.024	0.191	0.256	Hydroxy acids
Plasma				
L-Tyrosine	0.013	0.596	1.083	Amino acids
L-Ornithine	0.030	0.904	1.099	Amino acids
Tryptophan	0.036	0.904	1.100	Amino acids

†Palmitoleic acid	0.036	0.904	0.755	Fatty acids

†microbial metabolites

Changes in carbohydrates, amino acids, and fatty acids were correlated with gut microbiota

To investigate functional changes in the gut microbiome using metabolites as mediators, correlation analysis was performed between gut microbiota and metabolites whose relative abundance significantly changed at the metformin period. The carbohydrates, amino acids, hydroxy acids, and fatty acids were correlated with the microbiome (Figure 7). The *Intestinibacter* was positively correlated with urinary carbohydrates. The *Intestinibacter* and *Clostridium* were positively correlated with urinary amino acids (Figure 7a). In urinary metabolic markers, D−galactose, glyceric acid, glycolic acid, and 2,4−dihydroxybutyric acid were positively correlated with the *Intestinibacter, Clostridium,* and *Romboutsia*. In contrast, hypoxanthine and hippuric acid were negatively correlated with the *Intestinibacter, Clostridium,* and *Romboutsia*. In the correlation of stool metabolic markers and microbiome, essential amino acids such as phenylalanine and L−isoleucine were negatively correlated with the *Intestinibacter*, *Clostridium*, and *Romboutsia*. The three genera were positively correlated with carbohydrates, fatty acids, hydroxy acids, and L−serine, which are classified as nonessential amino acids (Figure 7b). For plasma metabolic markers, amino acids were positively correlated with

the genera, and palmitoleic acid was positively correlated with *Escherichia* (Figure 7c).

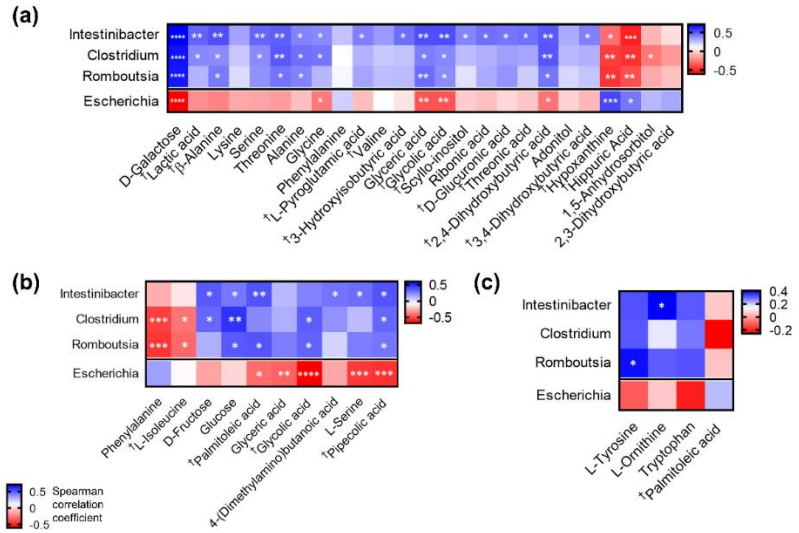

Figure 7. Heatmap showed the Spearman correlation coefficient between the relative abundances of individual microbial genera and the relative abundances of (a) urinary metabolite, (b) fecal metabolite, and (c) plasma metabolite. The y-axis represents the microbial genus, and the x-axis represents metabolites. The intensity of the colors represents the degree of the association. †microbial metabolites. *p-value < 0.05, **p-value < 0.005, ***p-value < 0.001, ****p-value < 0.0001.

Changed metabolites were correlated with the hypoglycemic effect

A correlation analysis was performed to determine whether changes in the PD parameters of metformin correlated with changes in metabolites (Figure 8). The PD parameters were positively correlated with urinary metabolic markers except for β-alanine and lysine (Figure 8a). The

stool amino acids were weakly positively correlated with the PD parameters, and carbohydrates were negatively correlated with the PD parameters (Figure 8b). Plasma metabolic markers were positively correlated with the PD parameters except for L-tyrosine (Figure 8c).

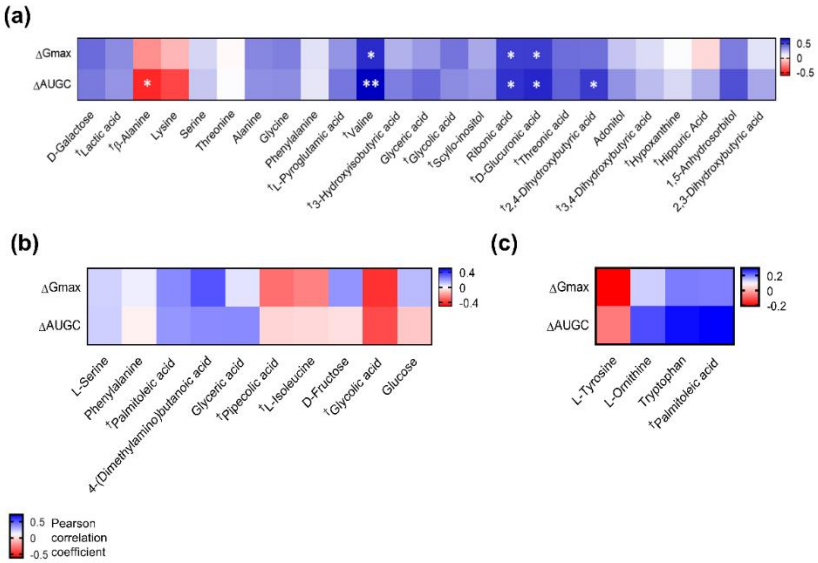

Figure 8. Pearson correlation analysis was performed to investigate the association between PDs ($\triangle G_{max}$ and $\triangle$AUGC) and (a) urinary metabolites, (b) fecal metabolites, and (c) plasma metabolites. The y-axis represents PDs, and the x-axis represents metabolites. Each square shows the correlation coefficient value. Blue squares indicate a positive correlation and red squares indicate a negative correlation. †microbial metabolites. *p-value < 0.05, **p-value < 0.005.

Changed metabolites were involved in gluconeogenesis, amino acid metabolism, and carbohydrate metabolism

The changed metabolites after metformin administration were correlated with microbiome and hypoglycemic effects. Thus, a metabolite set enrichment analysis was performed to explore the potential pathways. As a result, the metabolites were involved in various metabolism. In addition, throughout pathway mapping analysis, networks between the metabolites involved in the metabolism were explored. In the network of urinary metabolites, carbohydrate metabolism and serine-glycine metabolism were altered by administration of metformin (Figure 9a). In addition, urinary and stool microbial metabolites were involved in branched-chain amino acid metabolism and gluconeogenesis (Figure 9b).

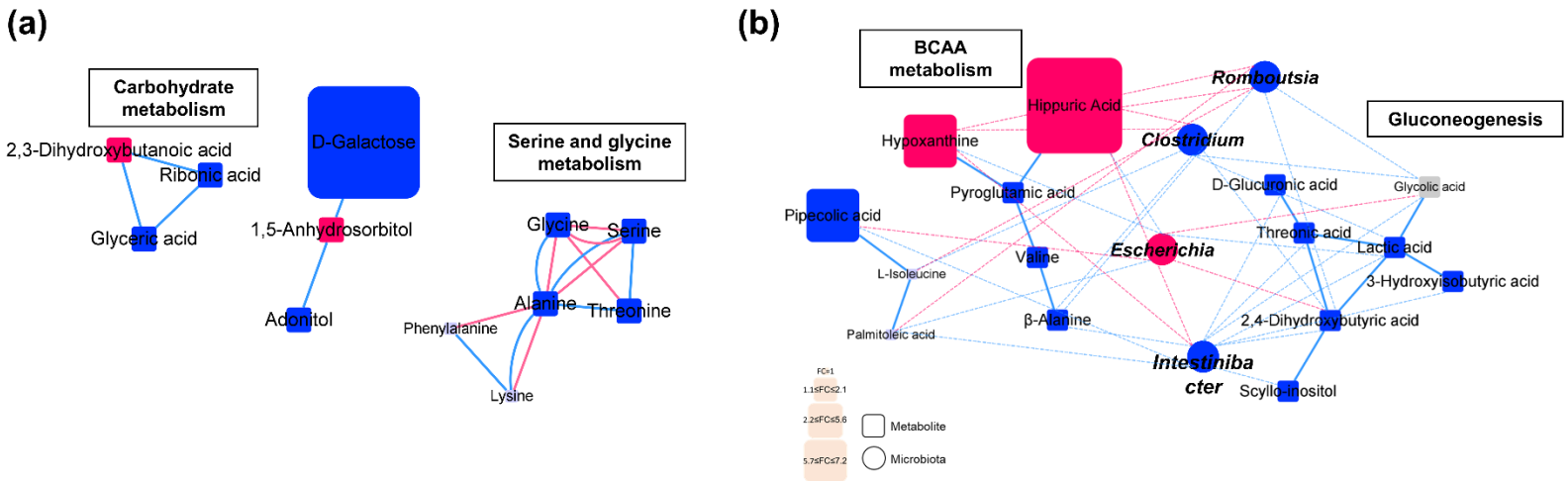

Figure 9. Metabolic correlation network diagram. (a) A fully connected network of metabolites detected in the urine samples. (b) Urinary and stool microbial metabolite correlation network diagram. The metabolites and microbiome are shown in color: red represents increase, blue represents decrease at metformin period, and gray represent no changes. The size of the nodes represents fold change of metabolites. The blue solid line represent chemical relationship and red solid line represent biochemical relationship. The red dashed line denotes negative correlation and blue dashed line denotes positive correlation.

Safety

Safety was evaluated in the 20 subjects administered metformin at least once. There were 15 adverse events (AEs) after administration of metformin. Of these AEs, 10 were gastrointestinal disorders. One case of diarrhea and one case of vomiting were evaluated as moderate AEs, and one case of vomiting was evaluated as a severe AE. All other AEs were mild.

STUDY Ⅱ. Changes in intestinal environment can impact pharmacodynamics of metformin through alterations in host metabolic pathways.

Demographics

A total of 15 healthy adult male subjects were enrolled in this study, with 14 subjects having completed the entire study after 1 subject withdrew consent. The mean ± standard deviation (SD) of the baseline demographic characteristics were as follows: age, 27.5 ± 6.23 years; height, 176.16 ± 7.51 cm; weight, 70.8 ± 11.69 kg; body mass index, 22.76 ± 2.96 kg/m^2.

Composition of microbial metabolites were altered by cholestyramine

Overall, the administration of cholestyramine markedly changed levels of microbial metabolites and their composition. In plasma bile acids, deoxycholic acid (DCA), glycoursodeoxycholic acid (GUDCA), and ursodeoxycholic acid (UDCA) were significantly reduced. While, glycocholic acid (GCA) and taurocholic acid (TCA) were significantly

increased after cholestyramine administration (Table 3). Regarding stool bile acids, the secondary bile acids such as DCA and lithocholic acid (LCA) were increased. The cholestyramine facilitated the excretion of secondary bile acids in stools. In addition, the plasma SCFAs, including butyrate, propionate, and valerate, were increased after cholestyramine administration (Table 3).

Table 3. Concentration of significantly changed bile acids and short-chain fatty acids (SCFA).

	Metformin (2d)	Cholestyramine+Metformin (9d)	FDR adjusted p-value
Plasma [μmol/L]			
DCA	0.28±0.2	0.11±0.09	0.0190
GUDCA	0.16±0.13	0.01±0.01	0.0067
UDCA	0.17±0.15	0.04±0.07	0.0122
GCA	0.19±0.3	1.07±0.78	0.0034
TCA	0.02±0.04	0.06±0.05	0.0350
Butyrate	0.93±0.46	1.54±0.66	0.0187
Propionate	0.41±0.23	0.67±0.41	0.0100
Valerate	0.29±0.08	0.39±0.09	0.0100
Stool [nmol/g]			
DCA	23.66±17.54	148.34±60.92	0.0004
LCA	16.53±10.78	58.96±39.59	0.0006

Data are presented as the arithmetic mean ± standard deviation. DCA, deoxycholic acid; GCA, glycocholic acid; GUDCA, glycoursodeoxycholic acid; TCA, taurocholic acid; UDCA, ursodeoxycholic acid; LCA, lithocholic acid.
FDR adjusted p-value: the paired t-test was used.

Bile acid sequestrant affects gut microbiota

A 16S rRNA sequencing was performed using stool samples. Alpha diversity did not change after administration of cholestyramine (p-value = 0.89, Mann-Whitney test for observed features; 0.14, Mann-Whitney test for Shannon index) (Figure 10a) and beta diversity based on the Bray-Curtis dissimilarity indices was used to evaluate the compositional dissimilarity (Figure 10b). Compared to the baseline, there were no overall changes in the beta diversity after cholestyramine administration (p-value < 0.748, PERMANOVA). Nevertheless, in linear discriminant analysis (LDA) coupled with effect size (LEfSe) analysis at the genus level, which is determining both statistical and biological relevance to discover a microbial biomarker, two genera were changed by cholestyramine administration. These included an increase in *Veillonella* and *Rothia* at genus level (FDR adjusted p-value < 0.1, LDA score > 2.0) (Figure 10c).

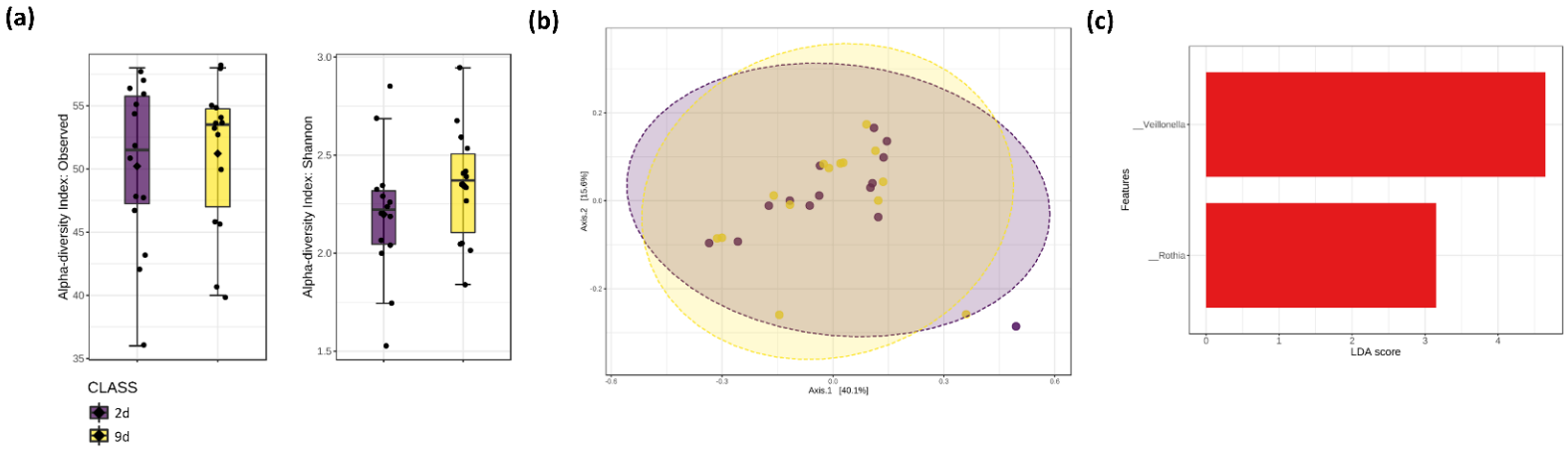

Figure 10. Changes in microbial composition following cholestyramine administration. (a) Alpha diversity was represented by observed features (OTUs) ($p = 0.89$, Mann–Whitney test) and Shannon index ($p = 0.14$, Mann–Whitney test). (b) Principal Coordinate Analysis (PCoA) plots showing beta diversity based on Bray–Curtis dissimilarity indices, which represents the dissimilarity of samples or groups. (c) Bacteria differentially represented between baseline and cholestyramine+metformin periods identified by linear discriminant analysis coupled with effect size (LEfSe). Histogram showing the genera of bacteria that were more abundant at cholestyramine+metformin period (FDR adjusted p-value < 0.1, LDA score > 2.0). The LDA score indicates the effect size and ranking of each differentially abundant genus. Violet: metformin period, Yellow: cholestyramine+metformin period. Box plots indicate the medians and the lower and upper quartiles. Each dot represents an individual sample.

Pharmacodynamics of metformin was affected by alterations in bile acids and gut microbiota

The serum glucose profiles and parameters at baseline and cholestyramine periods were similar, corresponding to the baseline of metformin and cholestyramine+metformin periods, respectively (Figure 11). There were no significant differences in systemic glucose levels represented by G_{max} and AUGC between baseline and cholestyramine periods (Table 5). After metformin administration, compared with baseline at each period, G_{max} and AUGC were decreased in metformin and cholestyramine+metformin periods, respectively (Table 4).

However, the absolute values of ΔG_{max} and ΔAUGC, which represent the pharmacodynamic effects of metformin, were lower in the cholestyramine+metformin period than in the metformin period. Moreover, a significant difference was detected for ΔAUGC, showing a %change of −44.7% in the cholestyramine+metformin period compared to the metformin period (p−value = 0.038) (Table 4).

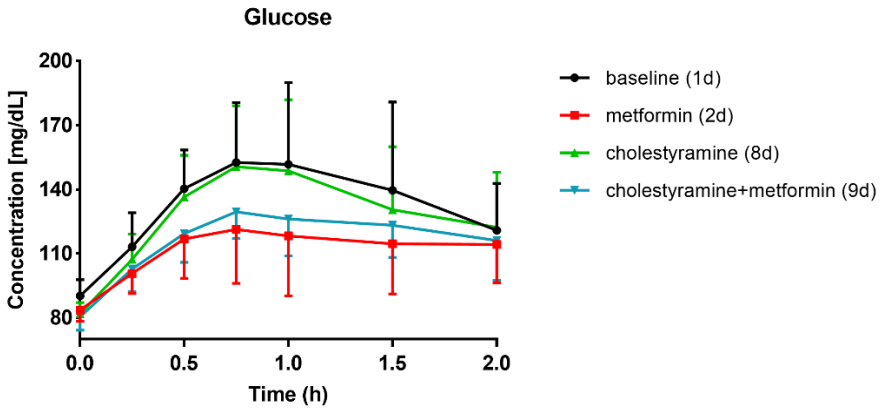

Figure 11. Mean serum glucose concentration-time profiles. Bars represent standard deviation. Metformin, administration of metformin alone; Cholestyramine, administration of cholestyramine alone; Metformin+Cholestyramine, co-administration of metformin and cholestyramine.

Table 4. Pharmacodynamics of metformin.

Parameters	Baseline	Metformin	Cholestyramine	Cholestyramine +metformin	%changes†	p-value*
Gmax (mg/dL)	162.21±31.51	131.36±21.84	157.79±29.86	134.36±14.44	-	
ΔGmax (mg/dL)	-	-30.86±16.79	-	-23.43±21.27	-24.1%	0.33
AUGC (h·mg/dL)	269.62±50.34	225.28±32.74	260.35±39.33	235.83±20.02	-	
ΔAUGC (h·mg/dL)	-	-44.34±25.76	-	-24.52±27.06	-44.7%	0.038*

Data are presented as the arithmetic mean ± standard deviation. G_{max}, maximum glucose concentration; AUGC, area under the glucose concentration curve from time 0 to the last measurable time point; ΔG_{max} and ΔAUGC obtained by calculating the value of 'metformin' - 'baseline' and 'cholestyramine+metformin' - 'cholestyramine', respectively.

*p-value: Paired t-test was used.

†Each ratio of changed value of PD parameters of 'cholestyramine+metformin' compared to corresponding value of 'metformin'.

Metformin altered endogenous metabolites

To explore changes in metabolic profiling after metformin administration, an untargeted metabolomics approach was performed. Serum and urine samples collected from all four periods were analyzed using GC−TOFMS. Overall, metabolic composition following metformin administration was observed to be different by alterations in bile acid and microbiota by cholestyramine. Especially, before alterations in bile acid and microbiota, carbohydrates and hydroxy acids were reduced in plasma by metformin administration. Also, urinary amino acids, carbohydrates, fatty acid, and hydroxy acids were reduced, except for citric acid (Table 5). These results were similar to those found in study Ⅰ.

However, after alterations in bile acid and microbiota, only alanine was significantly changed in plasma by metformin administration. In urinary metabolites, amino acids, carbohydrates, fatty acid, hydroxy acids, and uric acid were all reduced (Table 5).

Table 5. List of significantly changed metabolic markers.

Type	Name	p-value	FDR-adjusted p value	Fold Change	Class
Baseline vs. Metformin					
Plasma	Glyceric acid	0.00297	0.03022	0.81	Carbohydrate
	Threonic acid	0.00120	0.02204	0.80	Carbohydrate
	Glycolic acid	0.00328	0.03268	0.80	Hydroxy acid
	2-Hydroxybutyric acid	0.00490	0.03779	0.85	Hydroxy acid
	2,4-Dihydroxybutanoic acid	0.00005	0.00391	0.77	Hydroxy acid
Urine	Serine	0.00913	0.04076	0.74	Amino acid
	Glycine	0.00000	0.00014	0.69	Amino acid
	L-Lysine	0.01018	0.04448	0.60	Amino acid
	L-Threonine	0.00050	0.00484	0.31	Amino acids
	Glyceric acid	0.00785	0.03719	0.82	Carbohydrate
	1,5-Anhydrosorbitol	0.00301	0.01790	0.68	Carbohydrate
	Glutaric acid	0.00049	0.00484	0.20	Carboxylic acid
	Citric acid	0.00081	0.00671	1.26	Carboxylic acid
	Pimelic acid	0.00017	0.00260	0.47	Fatty acids
	Glycolic acid	0.00091	0.00711	0.79	Hydroxy acid
	2,4-Dihydroxybutanoic acid	0.00070	0.00618	0.72	Hydroxy acid
	3,4-Dihydroxybutanoic acid	0.00020	0.00275	0.72	Hydroxy acid
	Picolinic acid	0.00656	0.03282	0.74	Pyridine

Cholestyramine vs. Cholestyramine+Metformin

Plasma	L-Alanine	0.00605	0.03987	1.27	Amino acid
Urine	Serine	0.00030	0.00307	0.58	Amino acid
	Glycine	0.00081	0.00630	0.71	Amino acid
	Phenylalanine	0.00499	0.02276	0.67	Amino acid
	L-Lysine	0.00375	0.01804	0.51	Amino acid
	L-Histidine	0.00870	0.03377	0.61	Amino acid
	Glyceric acid	0.00424	0.01979	0.84	Carbohydrate
	1,5-Anhydrosorbitol	0.00174	0.01036	0.68	Carbohydrate
	Glucuronic acid	0.00912	0.03456	0.83	Carbohydrate
	L-Cysteine	0.00681	0.02780	0.58	Carboxylic acid
	Pimelic acid	1.5.E-07	0.00002	0.33	Fatty acids
	Glycolic acid	0.00104	0.00730	0.78	Hydroxy acid
	2,4-Dihydroxybutanoic acid	0.00115	0.00790	0.80	Hydroxy acid
	3,4-Dihydroxybutanoic acid	0.00001	0.00026	0.69	Hydroxy acid
	Uric acid	4.0.E-06	0.00011	0.02	Purine

Alteration in bile acids, gut microbiota, metabolites, and metformin pharmacodynamics were correlated

A correlation analysis was performed to identify the potential connections of the changes in bile acids, microbiota, metabolites, and metformin PDs. Firstly, there was found strong association between PD parameters and metabolites in the metformin period (Figure 12a). In particular, glucose parameters were correlated with 2-hydroxybutanoic acid, 2,4-dihydroxybutanoic acid, glycine, L-lysine, and citric acid. Moreover, the changes in BA and microbiota were correlated with both glucose parameters and changes in metabolites (Figure 12b). The changes in the relative abundance of *Romboutsia* and *Veillonella* were negatively correlated with glucose parameters. Moreover, GUDCA and UDCA in plasma bile acids were positively correlated with the glucose parameters. However, plasma GCA, TCA, and stool bile acids were negatively correlated with the glucose parameters.

Furthermore, all changed urinary metabolites were positively correlated with glucose parameters, whereas plasma alanine was negatively correlated with glucose parameters. In addition, the relative abundance of the microbiome was negatively correlated with carbohydrates and hydroxyl acids.

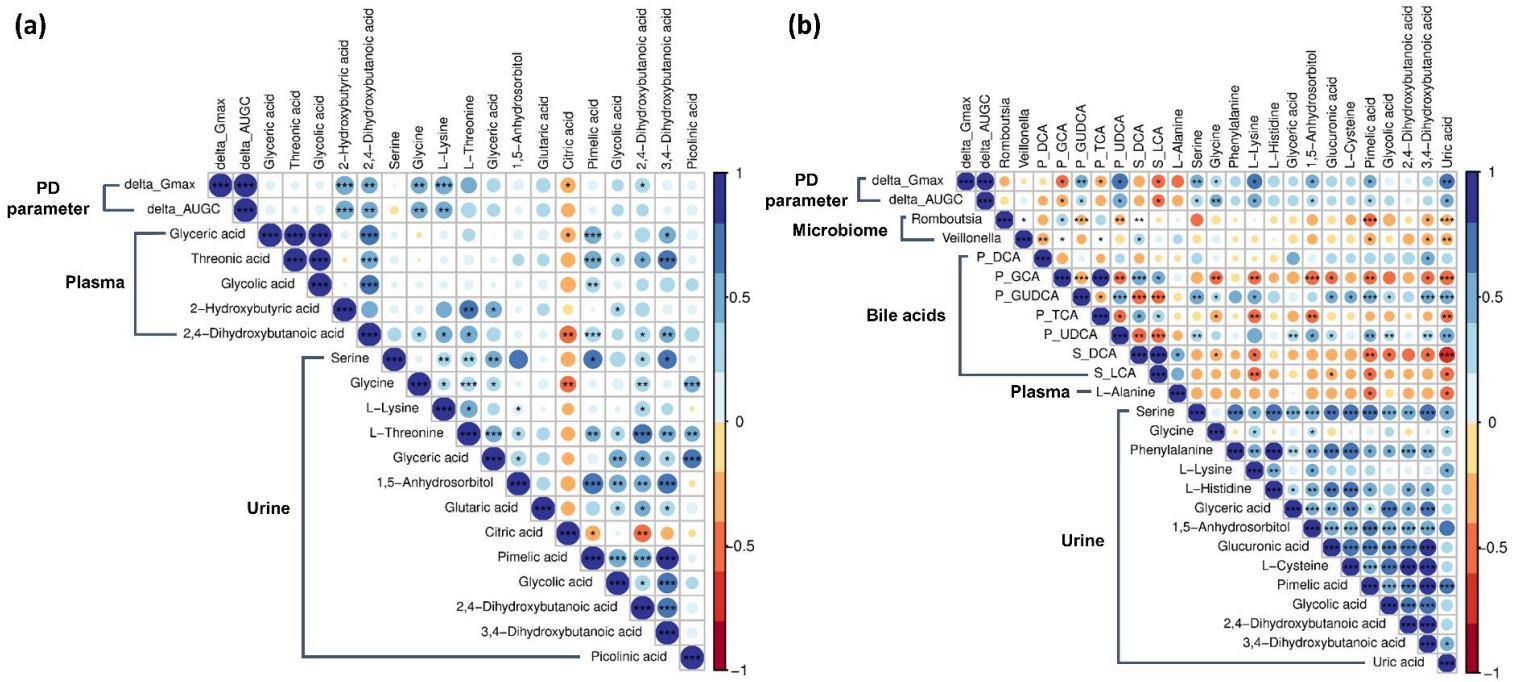

Figure 12. Spearman correlations between (a) baseline and metformin periods, and between (b) cholestyramine and cholestyramine+metformin periods. Circle size represents the correlation coefficient value. G_{max}, maximum glucose concentration; AUGC, area under the glucose concentration curve from time 0 to the last measurable time point; P_, bile acids from plasma; S_, bile acids from stool. Blue color indicates a positive correlation and red color indicates a negative correlation. *p−value < 0.05, **p−value < 0.01, ***p−value < 0.001.

The metabolic pathways that correlated with hypoglycemic effect were affected by bile acids composition.

A pathway analysis was performed and network was depicted to interrogate metabolic pathways related to hypoglycemia. Interestingly, glycine–serine metabolism was similarly altered by metformin administration regardless of changes in bile acids and the microbiome (Figure 14a). In normal state, propionate metabolism and TCA cycle were changed by metformin administration. In contrast, after changes in bile acids and microbiome, bile acid biosynthesis, amino acid metabolism, and purine metabolism were changed by metformin administration (Figure 14b).

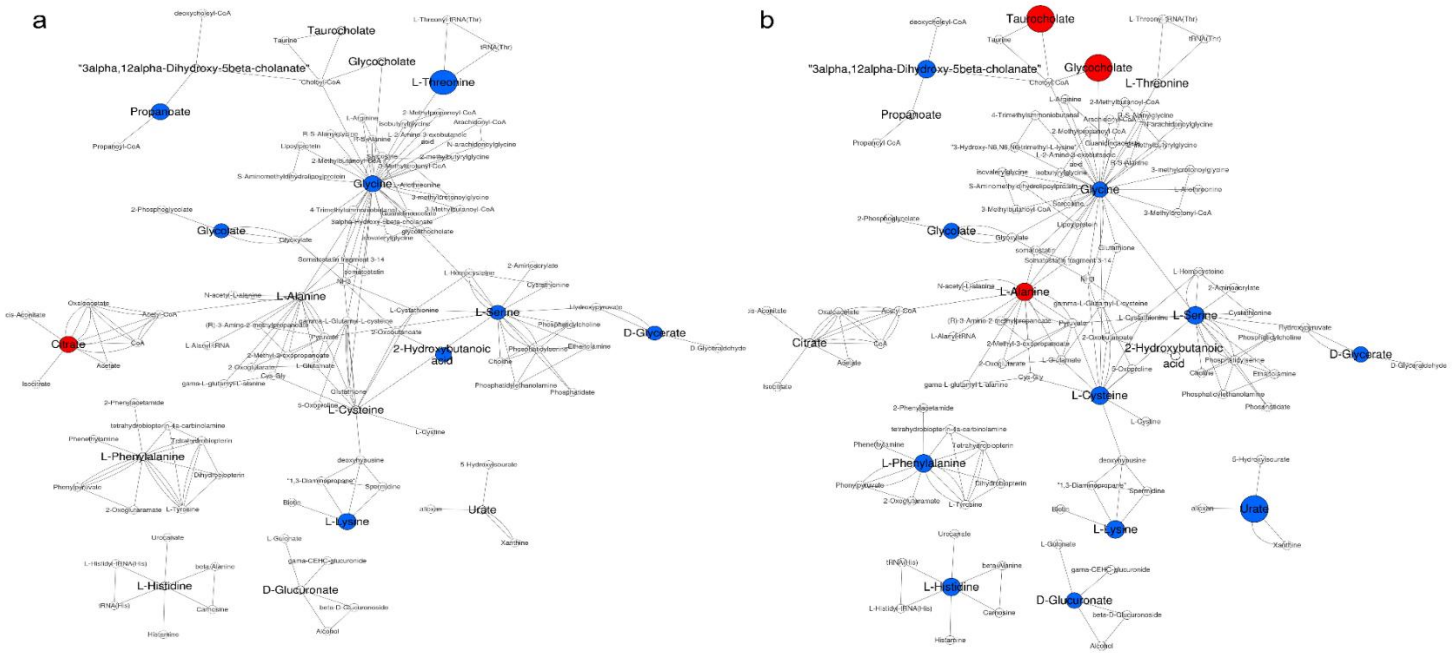

Figure 13. Metabolic networks of metabolic markers (a) between baseline and metformin periods and (b) between cholestyramine and cholestyramine+metformin periods. The metabolites were indicated by color: red represents increase, blue represents decrease, and white represents no change. The size of the nodes represents fold change and the solid line represents the relationship between the metabolites.

Discussion

These studies showed microbiota and metabolites that were changed by metformin and correlated with the hypoglycemic effect. In addition, it was identified that the changes in host's intestinal environment may affect the effectiveness of metformin (Figure 14).

Study Ⅰ was performed to identify changes in microbial composition and metabolites after metformin administration through metagenomic and metabolomic approaches. The subjects showed significant decreases in G_{max} and AUGC values, with a nonsignificant but trending decrease in the value of HOMA-IR. These results were supported by studies of metformin treatment in T2D patients unable to control blood glucose due to insulin resistance, preferentially regulating hepatic glucose output by inhibiting gluconeogenesis rather than controlling insulin levels[19, 20].

In addition, the subjects who taking metformin for 4 days showed significant changes in microbial composition, which was consistent with the results reported in T2D patients treated with metformin for 3 days [2]. Especially, the changes in various microbiome such as *Akkermansia*, *Escherichia*, *Intestinibacter*, *Clostridium*, and *Romboutsia* were observed, which was consistent with the results reported in previous studies [1, 11, 21]. The changes in *Akkermansia* were

observed after taking metformin but were not significant. The change in the relative abundance of *Escherichia* is assumed to be indirectly affected by bacteria–bacteria interactions or other physiological alterations [1]. Indeed, *Escherichia* was positively correlated with the hypoglycemic effect. The *Escherichia* could use glucose as a carbon source in the β–alanine pathway [22], and the increase in *Escherichia* was found to be related to improved glucose homeostasis by the regulation of metabolism, such as carbon uptake, catabolism, and energy and redox production [11, 23]. In fact, rats that underwent Roux–en–Y gastric bypass (RYGB) surgery to treat obesity had increased *Escherichia* and decreased glucose levels. Similarly, mice that underwent ileal interposition (IT) surgery to treat T2D had the same results [24, 25]. Therefore, an increase in the relative abundance of *Escherichia* after administration of metformin may contribute to improving the hyperglycemic effect.

The growth of *Firmicutes*, including *Intestinibacter*, *Clostridium*, and *Romboutsia*, was impeded by metformin [11, 21]. In addition, a decrease in *Firmicutes* has been reported to decrease insulin resistance and other factors that lead to the development of T2D [26]. *Intestinibacter*, *Clostridium*, and *Romboutsia*, belonging to *Firmicutes*, were negatively related to the hypoglycemic effect. *Firmicutes* can generate surplus energy from carbohydrates by fermenting unabsorbed

carbohydrates, and the accumulation of surplus energy can cause obesity and T2D [27]. In an animal study, *Firmicutes* were increased in *ob*/*ob* mice, and body fat mass and energy harvesting ability were increased in germ-free mice transplanted with *ob*/*ob* microbiomes, such as *Firmicutes* [28]. Thus, hyperglycemia may be improved as the relative abundance of *Firmicutes* decreases after administration of metformin.

The untargeted metabolomic analysis was used to explore the underlying pathway of the hypoglycemic effect in the study Ⅰ. The untargeted metabolomic analysis showed changes in metabolic signatures, including amino acid, carbohydrate, and fatty acid metabolism. In particular, amino acids, hippuric acid, glyceric acid, galactose, and palmitoleic acid were largely changed by administration of metformin. The hippuric acid, largely increased by administration of metformin, is a normal urinary component derived from the degradation of phenols and aromatic amino acids by a range of microbiome [29]. The level of hippuric acid decreased in obese patients and increased approximately 30-fold in patients who underwent RYGB surgery [29] and was also associated with impaired glucose tolerance [30]. Additionally, the decrease was reduced in T2D patients after treatment with antidiabetic drugs, which is correlated with a protective effect on gut microbiota metabolism [31]. The intermediates of energy

metabolism were altered after administration of metformin. In previous studies, myo-inositol, the bio-converted form of scyllo-inositol, is known to be elevated in T2D patients [32]. The high level of myo-inositol is due to competitive inhibition with glucose in renal tubular transport, and the level was decreased after administration of antidiabetic drugs. Thus, both the levels of myo-inositol and scyllo-inositol are expected to be good indicators of T2D treatment by antidiabetic drugs. Fatty acids, including palmitoleic acid, were increased in gestational diabetes mellitus patients. In particular, palmitoleic acid, produced by desaturation of palmitic acid, promotes gluconeogenesis [33]. In this study, the changes in these metabolites may affect the hypoglycemic effect of metformin.

In terms of the comprehensive metabolic effects on hypoglycemia, amino acid metabolism, fatty acid β-oxidation, and BCAA metabolism were important metabolic pathways. First, amino acid metabolism, such as serine-glycine metabolism, influences signaling associated with obesity and insulin resistance [34]. In particular, mammalian target of rapamycin complex (mTORC), which has been implicated in specific human pathologies, including obesity, T2D, and cancer, is affected by amino acid metabolism [35, 36]. Metformin inhibits mTORC1, which reduces ATP levels and activates AMPK [37], but amino acids stimulate mTORC1 signaling by activating a family of GTPases [38].

Therefore, a decrease in amino acids could affect mTORC1 signaling, thereby lowering blood glucose levels through the regulation of AMPK.

Moreover, AMPK activation can also affect fatty acid β-oxidation [39]. Fatty acid β-oxidation, the first step of fatty acid catabolism, is an energy production process. In T2D patients, fatty acid β-oxidation was decreased and associated with insulin resistance by impaired β-cell function [40]. Under this condition, more fatty acids were metabolized to more diacylglycerols, which inhibited the interaction between insulin and glucose transporter type 4 (GLUT4) [41]. Peroxisome proliferator-activated receptor-gamma (PPAR-γ) is a nuclear receptor that regulates fatty acid metabolism and glucose metabolism [42], and it is known to be activated by metformin [43]. The activation of AMPK by metformin induces PPAR-γ activity, which plays an important role in the transcriptional control of mitochondrial fatty acid β-oxidation by upregulating the expression of genes involved in fatty acid β-oxidation [39, 43].

BCAA metabolism could be affected by *Escherichia*, which contributes to an increase in BCAA biosynthesis and a reduction in BCAA transport into bacterial cells [44]. However, the role of BCAA is still controversial. On the one hand, insulin resistance is related to increased levels of BCAAs [44], but on the other hand, glucose homeostasis and insulin sensitivity are improved in mice fed a diet

enriched in leucine [45]. We confirmed that the hypoglycemic effect is influenced by BCAAs and *Escherichia*.

Additionally, to determine the effect of changes in the intestinal environment on the pharmacodynamics of metformin, study Ⅱ was conducted and explored the relationship between the microbiome, microbial metabolites, and the hypoglycemic effect of metformin. There was identified that the hypoglycemic effect of metformin was related to the alteration in microbial taxonomy and their metabolites, as well as endogenous metabolites.

In addition to the changes of total plasma bile acids by cholestyramine, plasma bile acid profiling presented a significant shift toward a more hydrophobic configuration. These hydrophobic bile acids were negatively correlated with hypoglycemic effect. Indeed, the hydrophobic bile acids increased in *ob/ob* mice [46] and high concentration of hydrophobic bile acids are known to be related with cytotoxicity [47]. Especially, the increases in plasma GCA and TCA which belong to hydrophobic bile acids, were related with metabolic diseases. In bile acid profiling of obese subjects, the GCA and TCA were higher in the subjects with HOMA-IR above the median value than those with HOMA-IR below the median value [48]. In addition, previous studies in both *in vitro* and in rats suggested that TCA elevates

secretin-stimulated cAMP levels, and the elevation induces hepatic gluconeogenesis [49].

In contrast, hydrophilic bile acids such as GUDCA and UDCA were positively correlated with the hypoglycemic effect. In the study, GUDCA and UDCA were reduced, and these bile acids belonged to both the FXR and TGR5 agonist, including DCA. The changes are supported by previous works in both mice and humans. In the mice studies, FXR deficient ($FXR^{-/-}$) mice exhibited increased gluconeogenesis in the liver and impaired glucose tolerance [14, 50]. Also, a reduction of bile acids belonging to FXR agonist decreased energy expenditure, interpreted as weight gain and insulin resistance [51]. In treatments using a FXR agonist, blood glucose levels were decreased by inhibiting hepatic gluconeogenesis and improved glycogen synthesis and storage [14]. Moreover, Tsuchida, et al. showed an antidiabetic effect of UDCA using mice fed a high-fat diet. The UDCA treatment improves hepatic insulin resistance by reducing plasma glucose, plasma insulin, and HOMA IR [52].

Another bile acid receptor, TGR5, is activated by both GUDCA and DCA. While TGR5 depleted mice display both impaired glucose tolerance and decreased GLP-1 secretion, activation of TGR5 improves mitochondrial function and increases energy expenditure, and incretin secretion [53]. In addition, T2D patients treated using a TGR5

agonist had improved blood glucose levels [54]. Therefore, the changes in bile acids might be affecting the hypoglycemic effect of metformin.

Impacts of bile acids on the gut microbiome are complicated. The moderate changes at genus level and no differences in the alpha and beta diversity demonstrated a relatively stable gut microbial community of the subjects during cholestyramine administration, which was consistent with the results obtained from icteric primary biliary cholangitis patients treated with cholestyramine [55]. Nevertheless, LEfSe analysis provided significant microbial changes at genus level. It is worth noting that the abundance of two genus, including *Rothia* and *Veillonella*, were significantly increased by cholestyramine administration and these microbiomes were negatively correlated with the hypoglycemic effect.

Rothia and *Veillonella* are known to the oral microbiota but present at relatively low abundances in the gut. In addition, they are sensitive to bile acid and hydrolyze bile acid conjugates to primary bile acids [56, 57]. Also, they tend to increase in disease groups [58–60]. The *Rothia* genera is increased in relative abundance in high-fat diet fed rats and correlated with both fasting glucose and insulin [61]. Moreover, the predominant *Rothia* is associated with elevated expression of carnitine acetyltransferase (*CRAT*). The *CRAT* converts acetyl-CoA to the acetylcarnitine in fatty acid oxidation and it is suggested to play a role

in the upregulation in insulin-resistant states[61, 62]. The *Veillonella* genus, which belongs to *Firmicutes* phylum, is gram-negative and known as a harmful bacteria [63]. In obese patients, the *Veillonella* was significantly increased in the high insulin-resistance group and found to be positively correlated with pro-inflammatory factors [64]. The microbiota is able to ferment lactate to propionate and acetate, but these SCFA do not induce mucin synthesis, which could result in an increase in gut permeability. This situation is able to induce insulin resistance and decrease secretion of intestinal hormones, such as GLP-1 and PYY, controlling glucose homeostasis [65].

However, it has been suggested that subtle alterations in microbial composition was able to shift microbial function profoundly. As microbial metabolites were considered as readouts of microbial function, targeted metabolomics was carried out to further explore the profiling of microbial metabolites. Interestingly, SCFA, including butyrate, propionate, and valerate were increased by cholestyramine. It has been reported in animal models fed high-fat diets that cholestyramine administration could increase the SCFA [66, 67]. This increase was associated with an increased ratio of *Firmicutes* to *Bacteroidetes* [28]. In addition, the increased valerate promotes intestinal energy harvesting and supports the development of metabolic disease [68].

Finally, the untargeted metabolomic profiling of endogenous metabolites was performed to understand how alterations in bile acids, microbiota, and microbial metabolites affect the hypoglycemic effect of metformin from mechanistic perspective. After the alteration, changes of the endogenous metabolites by metformin administration were different from those before the alteration. Specifically, changes involved in TCA cycle and purine metabolism. The TCA cycle is inhibited by metformin, which reduces production of ATP and elevating the hypoglycemic effect [37]. Moreover, citric acid, an intermediator of TCA cycle, tended to decrease in plasma (data not shown) but urinary citric acid was significantly increased. The citric acid level is regulated by metformin and a reduction in citric acid levels may be caused by an antidiabetic effect. Therefore, levels of citric acid were suggested as an indicator to observe the antidiabetic effect of metformin treatment in diabetic fatty rats [69].

The urinary uric acid, an intermediator of purine metabolism, was significantly reduced after the combination of cholestyramine and metformin. Serum uric acid has been reported to positively correlate with the risk of T2D and is suggested as a biomarker of T2D [70, 71]. Also, as serum uric acid acts as an oxidant in the environment of T2D [72], an increase in serum uric acid causes oxidative stress, predisposing individuals to the risk of T2D [73]. The serum uric acid

levels tend to be inversely proportional to urinary uric acid levels [74]. Thus, the increase in urinary uric acid may interfere with the hypoglycemic effect of metformin.

In these studies, paired samples were used to reduce the effect of inter-individual variations, a common issue in previous studies exploring the effect of metformin on the human gut microbiome [1, 11, 75, 76]. Additionally, because diet is a major modifiable factor influencing the microbial composition, the subjects of study I were hospitalized and fed the same diet for 2 days prior to starting metformin administration to reduce the effect of dietary intake on the human gut microbiome. As the microbial diversity can be altered short-term, dramatic dietary intervention [77], the dietary intervention might be sufficient to match between microbial composition in subjects prior to start the study. Thus, the design of the study enabled to decrease the effect of confounding factors that have an impact on the human gut microbiome.

Moreover, these studies revealed the underlying pathway of the hypoglycemic effect of metformin within the gastrointestinal tract through metagenomic and metabolomic approaches utilizing plasma, urine, and stool samples from healthy Korean subjects. However, these studies have some limitations. First, the suggested metabolic markers and the proposed pathway of the hypoglycemic effect has been

presented only as a correlation. In particular, further studies are needed on the role of microbial metabolites as intermediators between gut microbiome and hypoglycemia. Second, the clinical trials were conducted on Korean adults who were provided a normal diet, not a high-fat/high-fiber diet, to reduce the effect of diet on the results. Nevertheless, the human gut microbiota is affected by genetic and environmental factors, including diet, medications, and stress [78], and varies across different ethnic groups. Thus, further evaluation is needed in different ethnic groups with different diets. Third, the stool samples were not collected to validate the effect of metformin on microbial composition in study Ⅱ. Therefore, it was difficult to validate microbial change in study Ⅰ.

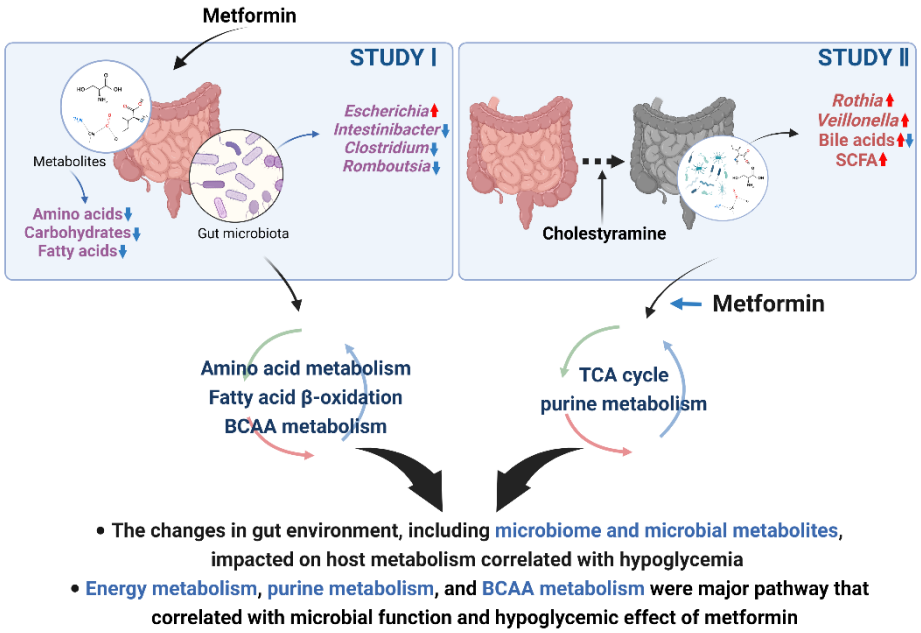

Figure 14. Summary of study Ⅰ and study Ⅱ.

Conclusion

In conclusion, these studies provided an interesting perspective into the hypoglycemic effect of metformin in the intestine through analyzing the changes of microbial composition and metabolites.

The alterations found within the gut environment, including microbiome and microbial metabolites, impacted on the hypoglycemic effect. Especially, amino acid metabolism, TCA cycle, BCAA metabolism, and purine metabolism were changed and correlated with the hypoglycemic effect. Therefore, as the mechanism of the hypoglycemic effect in the intestine has not been elucidated, it is noteworthy that these studies suggest potential pathways to correlate with the hypoglycemic effect.

References

1. Wu, H., et al., *Metformin alters the gut microbiome of individuals with treatment-naive type 2 diabetes, contributing to the therapeutic effects of the drug.* Nature medicine, 2017. **23**(7): p. 850-858.
2. Sun, L., et al., *Gut microbiota and intestinal FXR mediate the clinical benefits of metformin.* Nature medicine, 2018. **24**(12): p. 1919-1929.
3. Rena, G., D.G. Hardie, and E.R. Pearson, *The mechanisms of action of metformin.* Diabetologia, 2017. **60**(9): p. 1577-1585.
4. Zhou, G., et al., *Role of AMP-activated protein kinase in mechanism of metformin action.* The Journal of clinical investigation, 2001. **108**(8): p. 1167-1174.
5. Graham, G.G., et al., *Clinical pharmacokinetics of metformin.* Clinical pharmacokinetics, 2011. **50**(2): p. 81-98.
6. Bailey, C., C. Wilcock, and J. Scarpello, *Metformin and the intestine.* Diabetologia, 2008. **51**(8): p. 1552.
7. Bonora, E., et al., *Lack of effect of intravenous metformin on plasma concentrations of glucose, insulin, C-peptide, glucagon and growth hormone in non-diabetic subjects.* Current medical research and opinion, 1984. **9**(1): p. 47-51.
8. Buse, J.B., et al., *The primary glucose-lowering effect of metformin resides in the gut, not the circulation: results from short-term pharmacokinetic and 12-week dose-ranging studies.* Diabetes care, 2016. **39**(2): p. 198-205.
9. Shin, N.-R., et al., *An increase in the Akkermansia spp. population induced by metformin treatment improves glucose homeostasis in diet-induced obese mice.* Gut, 2014. **63**(5): p. 727-735.

10.Napolitano, A., et al., *Novel gut-based pharmacology of metformin in patients with type 2 diabetes mellitus.* PloS one, 2014. **9**(7): p. e100778.

11.Forslund, K., et al., *Disentangling type 2 diabetes and metformin treatment signatures in the human gut microbiota.* Nature, 2015. **528**(7581): p. 262-266.

12.Schroeder, B.O. and F. Bäckhed, *Signals from the gut microbiota to distant organs in physiology and disease.* Nature medicine, 2016. **22**(10): p. 1079-1089.

13.Matsubara, T., F. Li, and F.J. Gonzalez, *FXR signaling in the enterohepatic system.* Molecular and cellular endocrinology, 2013. **368**(1-2): p. 17-29.

14.Ma, K., et al., *Farnesoid X receptor is essential for normal glucose homeostasis.* The Journal of clinical investigation, 2006. **116**(4): p. 1102-1109.

15.Yamagata, K., et al., *Bile acids regulate gluconeogenic gene expression via small heterodimer partner-mediated repression of hepatocyte nuclear factor 4 and Foxo1.* Journal of Biological Chemistry, 2004. **279**(22): p. 23158-23165.

16.Mudaliar, S., et al., *Efficacy and safety of the farnesoid X receptor agonist obeticholic acid in patients with type 2 diabetes and nonalcoholic fatty liver disease.* Gastroenterology, 2013. **145**(3): p. 574-582. e1.

17.Ríos-Covián, D., et al., *Intestinal short chain fatty acids and their link with diet and human health.* Frontiers in microbiology, 2016. **7**: p. 185.

18.Sanna, S., et al., *Causal relationships among the gut microbiome, short-chain fatty acids and metabolic diseases.* Nature genetics, 2019. **51**(4): p. 600-605.

19.Defronzo, R.A., N. Barzilai, and D.C. Simonson, *Mechanism of metformin action in obese and lean noninsulin-dependent diabetic subjects.* The Journal of Clinical Endocrinology & Metabolism, 1991. **73**(6): p. 1294-1301.

20.Stumvoll, M., et al., *Metabolic effects of metformin in non-insulin-dependent diabetes mellitus.* New England Journal of Medicine, 1995. **333**(9): p. 550-554.

21.Eliakim-Raz, N., et al., *Predicting Clostridium difficile infection in diabetic patients and the effect of metformin therapy: a retrospective, case-control study.* European Journal of Clinical Microbiology & Infectious Diseases, 2015. **34**(6): p. 1201-1205.

22.Oliveira, A., et al., *A kinetic model of the central carbon metabolism for acrylic acid production in Escherichia coli.* PLoS computational biology, 2021. **17**(3): p. e1008704.

23.Millard, P., K. Smallbone, and P. Mendes, *Metabolic regulation is sufficient for global and robust coordination of glucose uptake, catabolism, energy production and growth in Escherichia coli.* PLoS computational biology, 2017. **13**(2): p. e1005396.

24.Cummings, B.P., et al., *Bile-acid-mediated decrease in endoplasmic reticulum stress: a potential contributor to the metabolic benefits of ileal interposition surgery in UCD-T2DM rats.* Disease models & mechanisms, 2013. **6**(2): p. 443-456.

25.Liou, A.P., et al., *Conserved shifts in the gut microbiota due to gastric bypass reduce host weight and adiposity.* Science translational medicine, 2013. **5**(178): p. 178ra41-178ra41.

26.Aitken, J.D. and A.T. Gewirtz, *Toward understanding and manipulating the gut microbiota.* Nature Reviews Gastroenterology & Hepatology, 2013. **10**(2): p. 72-74.

27.Clarke, S.F., et al., *The gut microbiota and its relationship to diet and obesity: new insights.* Gut microbes, 2012. **3**(3): p. 186-202.
28.Turnbaugh, P.J., et al., *An obesity-associated gut microbiome with increased capacity for energy harvest.* nature, 2006. **444**(7122): p. 1027-1031.
29.Calvani, R., et al., *Gut microbiome-derived metabolites characterize a peculiar obese urinary metabotype.* International journal of obesity, 2010. **34**(6): p. 1095-1098.
30.Zhao, X., et al., *Metabonomic fingerprints of fasting plasma and spot urine reveal human pre-diabetic metabolic traits.* Metabolomics, 2010. **6**(3): p. 362-374.
31.Huo, T., et al., *Metabonomic study of biochemical changes in urinary of type 2 diabetes mellitus patients after the treatment of sulfonylurea antidiabetic drugs based on ultra-performance liquid chromatography/mass spectrometry.* Biomedical Chromatography, 2015. **29**(1): p. 115-122.
32.Hong, J.H., et al., *Urinary chiro-and myo-inositol levels as a biological marker for type 2 diabetes mellitus.* Disease markers, 2012. **33**(4): p. 193-199.
33.Bukowiecka-Matusiak, M., et al., *Lipid profile changes in erythrocyte membranes of women with diagnosed GDM.* Plos one, 2018. **13**(9): p. e0203799.
34.Adams, S.H., *Emerging perspectives on essential amino acid metabolism in obesity and the insulin-resistant state.* Advances in nutrition, 2011. **2**(6): p. 445-456.
35.Marshall, S., *Role of insulin, adipocyte hormones, and nutrient-sensing pathways in regulating fuel metabolism and energy homeostasis: a nutritional perspective of diabetes, obesity, and cancer.* Science's STKE, 2006. **2006**(346): p. re7-re7.

36.Dann, S.G., A. Selvaraj, and G. Thomas, *mTOR Complex1–S6K1 signaling: at the crossroads of obesity, diabetes and cancer.* Trends in molecular medicine, 2007. **13**(6): p. 252–259.

37.Hardie, D.G., *Role of AMP–activated protein kinase in the metabolic syndrome and in heart disease.* FEBS letters, 2008. **582**(1): p. 81–89.

38.Kim, E., et al., *Regulation of TORC1 by Rag GTPases in nutrient response.* Nature cell biology, 2008. **10**(8): p. 935–945.

39.Lee, W.J., et al., *AMPK activation increases fatty acid oxidation in skeletal muscle by activating PPARα and PGC–1.* Biochemical and biophysical research communications, 2006. **340**(1): p. 291–295.

40.Wilding, J., *The importance of free fatty acids in the development of Type 2 diabetes.* Diabetic Medicine, 2007. **24**(9): p. 934–945.

41.Kraegen, E.W., G.J. Cooney, and N. Turner, *Muscle insulin resistance: a case of fat overconsumption, not mitochondrial dysfunction.* Proceedings of the National Academy of Sciences, 2008. **105**(22): p. 7627–7628.

42.Ahmadian, M., et al., *PPARγ signaling and metabolism: the good, the bad and the future.* Nature medicine, 2013. **19**(5): p. 557–566.

43.Mansour, H.H. and S.M. Galal, *Metformin and low dose radiation modulates cisplatin–induced oxidative injury in rat via PPAR–γ and MAPK pathways.* Archives of biochemistry and biophysics, 2017. **616**: p. 13–19.

44.Pedersen, H.K., et al., *Human gut microbes impact host serum metabolome and insulin sensitivity.* Nature, 2016. **535**(7612): p. 376–381.

45.Zhang, Y., et al., *Increasing dietary leucine intake reduces diet–induced obesity and improves glucose and cholesterol metabolism in mice via multimechanisms.* Diabetes, 2007. **56**(6): p. 1647–1654.

46.Li, T., et al., *Glucose and insulin induction of bile acid synthesis: mechanisms and implication in diabetes and obesity.* Journal of Biological Chemistry, 2012. **287**(3): p. 1861-1873.

47.Prawitt, J., S. Caron, and B. Staels, *Bile acid metabolism and the pathogenesis of type 2 diabetes.* Current diabetes reports, 2011. **11**(3): p. 160-166.

48.De Vuono, S., et al., *Serum bile acid levels before and after sleeve gastrectomy and their correlation with obesity-related comorbidities.* Obesity surgery, 2019. **29**(8): p. 2517-2526.

49.Glaser, S., et al., *Taurocholic acid prevents biliary damage induced by hepatic artery ligation in cholestatic rats.* Digestive and Liver Disease, 2010. **42**(10): p. 709-717.

50.Lefebvre, P., et al., *Role of bile acids and bile acid receptors in metabolic regulation.* Physiological reviews, 2009. **89**(1): p. 147-191.

51.Watanabe, M., et al., *Lowering bile acid pool size with a synthetic farnesoid X receptor (FXR) agonist induces obesity and diabetes through reduced energy expenditure.* Journal of Biological Chemistry, 2011. **286**(30): p. 26913-26920.

52.Tsuchida, T., et al., *Ursodeoxycholic acid improves insulin sensitivity and hepatic steatosis by inducing the excretion of hepatic lipids in high-fat diet-fed KK-Ay mice.* Metabolism, 2012. **61**(7): p. 944-953.

53.Thomas, C., et al., *TGR5-mediated bile acid sensing controls glucose homeostasis.* Cell metabolism, 2009. **10**(3): p. 167-177.

54.Keitel, V., R. Kubitz, and D. Häussinger, *Endocrine and paracrine role of bile acids.* World journal of gastroenterology: WJG, 2008. **14**(37): p. 5620.

55.Li, B., et al., *Alterations in microbiota and their metabolites are associated with beneficial effects of bile acid sequestrant on icteric primary biliary Cholangitis.* Gut microbes, 2021. **13**(1): p. 1946366.
56.Aries, V., et al., *Degradation of bile salts by human intestinal bacteria.* Gut, 1969. **10**(7): p. 575.
57.Loomba, R., et al., *The Commensal Microbe V eillonella as a Marker for Response to an FGF19 Analog in NASH.* Hepatology, 2021. **73**(1): p. 126-143.
58.Friedman, E.S., et al., *FXR-dependent modulation of the human small intestinal microbiome by the bile acid derivative obeticholic acid.* Gastroenterology, 2018. **155**(6): p. 1741-1752. e5.
59.Ni, J., et al., *Analysis of the relationship between the degree of dysbiosis in gut microbiota and prognosis at different stages of primary hepatocellular carcinoma.* Frontiers in microbiology, 2019. **10**: p. 1458.
60.Wei, W., et al., *Altered metabolism of bile acids correlates with clinical parameters and the gut microbiota in patients with diarrhea-predominant irritable bowel syndrome.* World Journal of Gastroenterology, 2020. **26**(45): p. 7153.
61.Kaakoush, N.O., et al., *Cross-talk among metabolic parameters, esophageal microbiota, and host gene expression following chronic exposure to an obesogenic diet.* Scientific reports, 2017. **7**(1): p. 1-10.
62.Adams, S.H., et al., *Plasma acylcarnitine profiles suggest incomplete long-chain fatty acid β-oxidation and altered tricarboxylic acid cycle activity in type 2 diabetic African-American women.* The Journal of nutrition, 2009. **139**(6): p. 1073-1081.

63.Ma, Q., et al., *Research progress in the relationship between type 2 diabetes mellitus and intestinal flora.* Biomedicine & Pharmacotherapy, 2019. **117**: p. 109138.

64.Moreno-Indias, I., et al., *Insulin resistance is associated with specific gut microbiota in appendix samples from morbidly obese patients.* American journal of translational research, 2016. **8**(12): p. 5672.

65.Burger-van Paassen, N., et al., *The regulation of intestinal mucin MUC2 expression by short-chain fatty acids: implications for epithelial protection.* Biochemical Journal, 2009. **420**(2): p. 211-219.

66.Alexander, C., et al., *Cholestyramine decreases apparent total tract macronutrient digestibility and alters fecal characteristics and metabolites of healthy adult dogs.* Journal of animal science, 2019. **97**(3): p. 1020-1026.

67.Kusumoto, Y., et al., *Bile acid binding resin prevents fat accumulation through intestinal microbiota in high-fat diet-induced obesity in mice.* Metabolism, 2017. **71**: p. 1-6.

68.Canfora, E.E., J.W. Jocken, and E.E. Blaak, *Short-chain fatty acids in control of body weight and insulin sensitivity.* Nature Reviews Endocrinology, 2015. **11**(10): p. 577-591.

69.Dong, Y., et al., *Urinary metabolomic profiling in Zucker diabetic fatty rats with type 2 diabetes mellitus treated with glimepiride, metformin, and their combination.* Molecules, 2016. **21**(11): p. 1446.

70.Dehghan, A., et al., *High serum uric acid as a novel risk factor for type 2 diabetes.* Diabetes care, 2008. **31**(2): p. 361-362.

71.Chien, K.-L., et al., *Plasma Uric Acid and the Risk of Type 2 Diabetes in a Chinese Community.* Clinical Chemistry, 2008. **54**(2): p. 310-316.

72.Hayden, M.R. and S.C. Tyagi, *Uric acid: A new look at an old risk marker for cardiovascular disease, metabolic syndrome, and type 2 diabetes mellitus: The urate redox shuttle.* Nutrition & metabolism, 2004. **1**(1): p. 1-15.

73.Odegaard, A.O., et al., *Oxidative stress, inflammation, endothelial dysfunction and incidence of type 2 diabetes.* Cardiovascular diabetology, 2016. **15**(1): p. 1-12.

74.Yuan, T., et al., *Effects of dapagliflozin on serum and urinary uric acid levels in patients with type 2 diabetes: a prospective pilot trial.* Diabetology & Metabolic Syndrome, 2020. **12**(1): p. 1-9.

75.Karlsson, F.H., et al., *Gut metagenome in European women with normal, impaired and diabetic glucose control.* Nature, 2013. **498**(7452): p. 99-103.

76.Zhernakova, A., et al., *Population-based metagenomics analysis reveals markers for gut microbiome composition and diversity.* Science, 2016. **352**(6285): p. 565-569.

77.David, L.A., et al., *Host lifestyle affects human microbiota on daily timescales.* Genome biology, 2014. **15**(7): p. 1-15.

78.Dave, M., et al., *The human gut microbiome: current knowledge, challenges, and future directions.* Translational Research, 2012. **160**(4): p. 246-257.

국문 초록

서론: 가장 널리 사용되는 항당뇨병 약물인 메트포르민은 간에서 AMP 매개 단백질 키나아제(AMPK)를 활성화시켜 지방산의 생합성과 포도당 생성을 억제하는 것으로 알려져 있지만, 최근들어 메트포르민이 장내 미생물군집에 영향을 미친다는 연구결과가 증가하고 있다. 일부 선행 연구에서는 메트포르민 투여 후 장내 미생물 조성 변화를 관찰하여 장내 미생물의 변화가 메트포르민의 혈당 저하 효과에 기여할 수 있음을 보고하였다. 하지만 현재까지 메트포르민의 장내 미생물군을 통한 혈당 강하 효과의 기전에 대해서는 분명하게 밝혀지지 않았다. 따라서, 본 연구에서는 건강한 성인 남성을 대상으로 진행한 두 개의 임상 연구를 통해 메트포르민이 장내에서 미치는 영향 및 다양한 상호작용에 대하여 파악하고 메타지노믹스와 메타볼로믹스 분석법을 활용하여 위장관을 통한 메트포르민의 혈당 강하 효과의 잠재적인 메커니즘을 설명하고자 하였다.

방법: 메트포르민이 장내 미생물군 및 대사산물에 미치는 영향을 평가하기 위해 20 명의 건강한 한국 남성을 대상으로 공개 및 단일군 임상 연구를 수행하였다. 연구 대상자들은 4 일 동안 하루에 두 번 경구 메트포르민 1000mg 을 복용하였다. 또한, 메트포르민의 혈당 강하 효과에 대한 미생물 대사 산물의 영향을 평가하기 위해 14 명의 건강한 한국 남성이 임상시험에 모집되었으며, 4 개의 시기(period)인 baseline(기저치), metformin(1-2 일째에 1000mg 메트포르민의 반복 경구투여), cholestyramine(장내 미생물군 및 미생물 유래 대사체의 전반적인 변화를

유도하기 위해 3-9 일째에 콜레스티라민 4g 의 반복 경구투여), cholestyramine + metformin(8-9 일째에 1000mg 메트포르민의 반복 경구투여)의 순서로 진행되었다. 두 임상 연구의 각 시기에는 혈청 포도당 및 인슐린 농도 측정을 위하여 경구 포도당 내성 검사 전후에 혈액 검체를 수집하였다. 또한, 장내 미생물 분석을 위한 대변 샘플, 대사체 분석을 위한 혈장, 소변 및 대변 검체를 수집하였으며, 메트포르민의 혈당 강하 효과의 잠재적 경로를 탐색하기 위해 네트워크 분석을 진행하였다.

결과: metformin 투여에 의해 *Escherichia*, *Romboutsia*, *Intestinibacter* 및 *Clostridium* 의 상대풍부도(relative abundance)가 변했으며, 탄수화물, 아미노산 및 지방산에 해당하는 대사체가 변했음을 확인했다. 이러한 장내 미생물군집 및 대사체의 변화는 메트포르민의 혈당 강하 효과와 상관관계를 보였다. 담즙산 격리제인 cholestyramine 투여에 의해 *Rothia* 와 *Veillonella* 의 상대풍부도가 증가하였고, 담즙산 및 단쇄 지방산과 같은 미생물 유래 대사체가 변했다. 이러한 변화는 메트포르민의 약력학 및 메트포르민 투여에 의해 변화된 내인성 대사체의 프로파일링에도 영향을 미쳤다. 또한, 네트워크 분석을 통해 메트포르민의 혈당 강하 효과와 관련된 주요 대사경로로 에너지 대사, 분지쇄 아미노산 대사, 퓨린 대사를 제시하였다.

결론: 본 연구를 통해 특정 장내 미생물군과 미생물 유래 대사체의 변화가 메트포르민의 혈당 강하 효과에 영향을 미친다는 것을 확인하였다. 이러한 변화들은 혈당 강하와 관련있는 숙주 대사에 영향을 미쳤다. 특히, 에너지 대사, 분지쇄 아미노산 대사 및 퓨린 대사가 메트포르민의 혈당강하

효과와 관련이 있었으며, 최종적으로 본 연구의 결과는 위장관을 통한 메트포르민의 잠재적인 기전을 밝히는 데 도움을 줄 수 있을 것으로 기대한다.

*본 내용의 일부는 Diabetes Research and Clinical Practice 학술지(Yujin Lee et al. *Diabetes Research and Clinical Practice* 178 (2021): 108985)에 출판 완료된 내용임.

주요어: 메트포르민, 제 2 형 당뇨병, 장내 미생물, 대사체학, 약력학

학 번: 2017-20297